DOI: 10.1002/chem.201000611

Design, Synthesis and Characterisation of a Fluorescently Labelled CyPLOS Ionophore**

Cinzia Coppola,[a] Antonio Paciello,[a] Gaetano Mangiapia,[b, c] Sabina Licen,[d] Mariangela Boccalon,[d] Lorenzo De Napoli,[a] Luigi Paduano,[b, c] Paolo Tecilla,[d] and Daniela Montesarchio*[a]

Abstract: A novel fluorescently labelled synthetic ionophore, based on a cyclic phosphate-linked disaccharide (CyPLOS) backbone and decorated with four tetraethylene glycol tails carrying dansyl units, has been synthesised in 12 steps in 26% overall yield. The key intermediate in the synthetic strategy is a novel glucoside building block, serving through its 2- and 3-hydroxy groups as the anchor point for flexible tetraethylene glycol tentacles with reactive azido moieties at their ends. To test the versatility of this glucoside scaffold, it was preliminarily functionalised with a set of diverse probes—as fluorescent, redox-active or hydrophobic tags—either by reduction of the azides followed by condensation with activated carboxylic acid derivatives, or by a direct coupling with a terminal alkyne in a Cu^{I}-promoted 1,3-dipolar cycloaddition. Tagging of the monomeric building block with dansyl residues allowed us to prepare a fluorescent, amphiphilic macrocycle, which was investigated for its propensity to self-aggregate in $CDCl_3$—studied by means of concentration-dependent ^{31}P NMR spectroscopy experiments—and in aqueous solution, in which combined dynamic light scattering (DLS) and small-angle neutron scattering (SANS) measurements provided a detailed physico-chemical analysis of the self-assembled systems, mainly organised in the form of large vesicles. Its ion-transport properties through phospholipid bilayers, determined by HPTS fluorescence assays, showed this compound to be more active than the previously synthesised CyPLOS congeners. Solvent-dependent fluorescence changes for the labelled ionophore in liposome suspension established that the dansyl moieties are dispersed in environments with polarity intermediate between those of CH_2Cl_2 and propan-2-ol, suggesting that the CyPLOS tentacles infiltrate the mid-polar region of the membranes.

Keywords: amphiphilic oligosaccharides · fluorescent probes · ion transport · macrocyclic compounds · self-assembly

Introduction

A wide number of diverse synthetic ionophores, functional analogues of ion channels or carriers, but typically displaying poor or no structural similarity with their natural, polypeptide-based counterparts, have been described in the recent literature.[1] Notwithstanding the large amounts of data collected on ion transport across cell membranes, promoted either by natural or by artificial agents, the overall picture of the structure–activity relationships is still not completely clear, with many different mechanisms of action being operative and with high ionophore efficiencies being exhibited both by very complex proteic architectures[2] and by structurally simple, small organic molecules.[3]

Suitably derivatised carbohydrates are ideal platforms for the construction of effective artificial receptors in molecular or ion recognition, because they are easily available starting materials, displaying multiple functional groups in well-de-

[a] Dr. C. Coppola, Dr. A. Paciello, Prof. L. De Napoli, Prof. D. Montesarchio
Department of Organic Chemistry and Biochemistry
University "Federico II" of Napoli
Via Cintia, 4, 80126 Napoli (Italy)
Fax: (+39) 081-674393
E-mail: daniela.montesarchio@unina.it

[b] Dr. G. Mangiapia, Prof. L. Paduano
Department of Chemistry "Paolo Corradini"
University "Federico II" of Napoli
Via Cintia, 4, 80126 Napoli (Italy)

[c] Dr. G. Mangiapia, Prof. L. Paduano
CSGI, Consorzio univ. per lo sviluppo
dei Sistemi a Grande Interfase (Italy)

[d] Dr. S. Licen, Dr. M. Boccalon, Prof. P. Tecilla
Department of Chemical Sciences
University of Trieste, Via L. Giorgieri
34127 Trieste (Italy)

[**] CyPLOS = Cyclic phosphate-linked oligosaccharide.

fined stereochemical presentations. These valuable synthetic scaffolds offer further advantages from the perspective of in vivo applications, playing pivotal roles in many cellular processes and showing favourable pharmacokinetic properties. In addition, when conjugated to valuable metabolites, they can confer resistance to enzymatic degradation and cell uptake enhancement, eliciting specific molecular recognition processes, mediated by membrane proteins (lectins).[4] For these and other reasons the development of glycoconjugates or hybrid backbones incorporating saccharide moieties is a research field in continuous development.[5]

Aiming at the preparation of novel macrocycles useful for specific ion recognition, we recently described the synthesis and conformational properties of a novel class of cyclic oligosaccharide analogues, 4,6-linked through stable phosphodiester bonds (**1**–**3**), that we named CyPLOSs (cyclic phosphate-linked oligosaccharide analogues).[6]

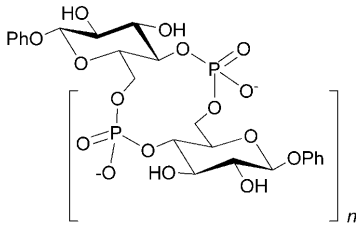

1 (*n*=1)
2 (*n*=2)
3 (*n*=3)

Amphiphilic macrocycles with remarkable propensities to aggregate were then obtained by attaching long tentacles with different hydrophobicities, particularly *n*-undecyl or benzyl-capped tetraethylene glycol (TEG) chains, to the CyPLOS backbones (**4**–**6**).[7]

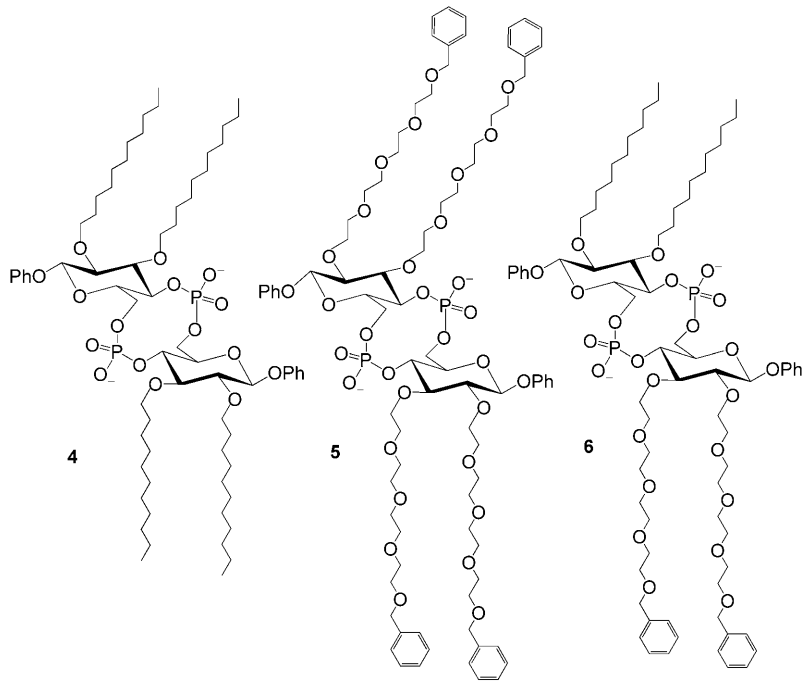

4 **5** **6**

Studies on the ionophoric activities of amphiphilic CyPLOSs[8] showed **5** to be the most effective compound in the investigated series, capable of discharging the pH gradient across a liposomial membrane completely in less than 20 min at 2% ionophore concentration. This property was strictly correlated to the presence of TEG chains, with **5** being much more active than **6** and the tetra-alkylated derivative **4** being almost completely inactive. Analysis of the ionophoric properties of **5** in comparison with those of its linear and fully protected cyclic congeners led us to the conclusion that both the four TEG tentacles and the fairly rigid anionic macrocycle are structural motifs essential for activity. When investigated for selectivity in ion transport, CyPLOS **5** did not show any significantly different behaviour with variation in the nature of the cation in solution; on the other hand, when tested with different anions, high transport activities were found with halogens (except fluoride), nitrate and perchlorate, whereas on the contrary, fluoride, acetate, glutamate and sulfate were not effectively transported. The lack of selectivity towards lipophilic anions was attributed to the formation of a poorly structured active species with little specificity towards the transported ions.

With the final objective of preparing novel and more efficient analogues of **5**, containing reporter groups that should in principle allow better insight into their mechanism of action, we first set out to investigate the synthesis of a versatile glucoside intermediate that would be susceptible to further derivatisation and widely applicable for the construction of multi-labelled architectures. For this purpose we designed the glucoside scaffold **8** (Scheme 1, below), bearing at its 2- and 3-OH positions flexible tetraethylene glycol chains connected at their ends to further reactive azido groups. This novel glucoside has been exploited to generate a small library of model labelled monosaccharides conjugated with different dyes (**10a**–**10c**, Scheme 3, below, and **12**, Scheme 4, below), to demonstrate its effective applicability. The building blocks **16** and **17** (Scheme 5, below) were then selected to generate the multi-labelled macrocycle **21** (Scheme 6, below), very similar to **5** except that the terminal benzyl groups are replaced by the fluorescent 5-*N*,*N*-dimethylaminonaphthalenesulfonyl (dansyl) residues. The use of fluorescent chemosensors as extremely powerful analytical and diagnostic tools, particularly for supramolecular applications, is widely documented in the recent literature.[9] Of the most commonly used fluorescent dyes, the dansyl group is considered an excellent probe for the

study of self-assembly or recognition processes, being dramatically sensitive to external stimuli or different environments.[10] Typically, it exhibits large solvent-dependent fluorescence shifts and has been inserted in several synthetic ion transporters to investigate their mechanism of action, also allowing easy monitoring of their incorporation in cells.[11] As a further advantage, it is chemically stable and can be easily conjugated to systems containing primary amines or hydroxy functions by direct coupling with its commercially available chloride derivative. Herein, we describe the synthesis and properties of the novel dansyl-labelled CyPLOS macrocycle **21**; a variety of analytical techniques were also exploited to study its self-assembly, partition, localisation within liposomes and its ionophoric activity, also in comparison with the previously synthesised congeners.

Results and Discussion

Synthesis of the versatile glucoside 8 and its conversion into the labelled derivatives 10a–10c and 12: The glucoside scaffold **8** (Scheme 1) is a highly versatile building block, characterised by two tetraethylene glycol appendages with azido residues at their ends. These groups, generally chemically stable, can be activated under appropriate conditions and coupled with a range of diverse labels, including fluorescent and/or electrochemically active probes. The derivative **8** can undergo high-yielding condensations through the exploitation of different but equally reliable synthetic schemes. As summarised in Scheme 1, two approaches have been adopted here. The first involves a two-step, one-pot reaction, requiring reduction of the azido groups to primary amines, followed by coupling with suitably activated derivatives of carboxylic acids, in a classical Staudinger ligation approach.[12] In the second strategy, glucoside **8** is exploited in a direct coupling with a terminal alkyne by means of the Cu^{I}-assisted azide–alkyne 1,3-dipolar cycloaddition (the so called "click-chemistry" approach).[13] This reaction owes its recent fortune to its compatibility with a broad range of functional groups and different solvent systems, including water. In addition, the newly generated triazole ring is stable to hydrolytic and enzymatic cleavage and is virtually inert to a variety of conditions. In all cases, the obtained functionalised glucosides provide novel amphiphilic scaffolds useful in the construction of carbohydrate-based receptors with peculiar spectroscopic properties, allowing easy detection of interaction events in molecular recognition.

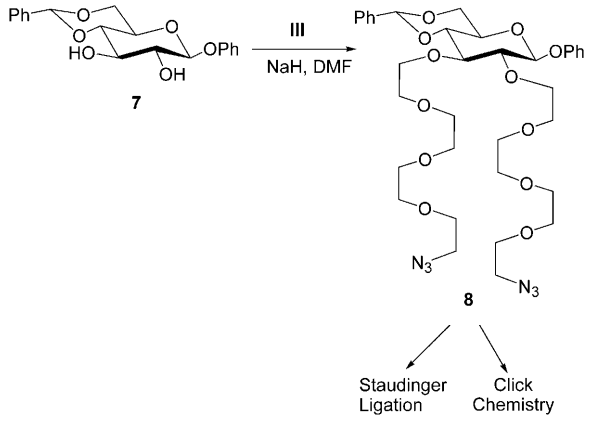

Scheme 1. General scheme for the synthesis and applications of the glucoside **8**.

The synthetic route to **8** first required the elaboration of tetraethylene glycol (TEG),[14] a flexible bifunctional linker widely used for the covalent attachment of dyes to biomolecules,[15] about 17 Å long in its fully extended conformation.[16] In our synthetic scheme, tetraethylene glycol was subjected to the following straightforward and high-yielding reactions (depicted in Scheme 2): monotosylation, azidation and activation of the free OH group as a mesyl ester. Once the activated monoazido-TEG **III** had been obtained[17] it was employed in a coupling with the 4,6-benzylidene-protected sugar **7** (Scheme 1) in a classical Williamson reaction, carried out in DMF in the presence of an excess of NaH, which allowed the persubstitution of the secondary 2- and 3-OH groups, leading to **8** in 90% yields.

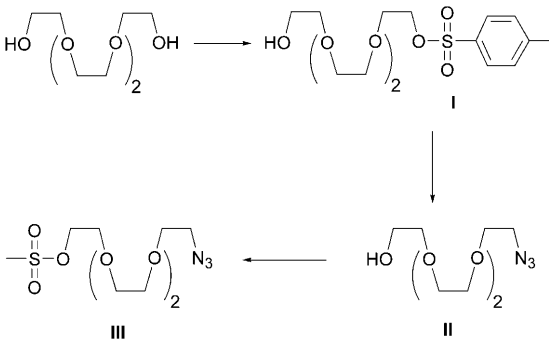

Scheme 2. Synthesis of the activated TEG-azido derivative **III**.

To demonstrate the feasibility of this synthetic strategy, glucoside **8** was functionalised with a selected panel of diverse labels, either by classical Staudinger ligation reactions or by the click chemistry approach. In the first synthetic investigation we prepared the derivatives **10a–10c**, each incorporating a fluorescent tag in the form of the 5-*N*,*N*-dimethylaminonaphthalenesulfonyl (dansyl) residue, an aromatic α-amino acid (i.e., 9-fluorenylmethoxycarbonyl (Fmoc)-protected tryptophan) and an electrochemically active probe (ferrocenecarboxylic acid), respectively (Scheme 3).

In a typical experiment, glucoside **8** was first treated with triphenylphosphine in water, followed by coupling of the freshly generated primary diamine **9** with the reactive tag in CH_2Cl_2 at room temperature. No condensing reagent was required for the coupling with dansyl chloride; in the cases of the derivatives **10b** and **10c**, dicyclohexylcarbodiimide (DCC) was adopted as the activating agent for the carboxylic acid functions. The reactions, monitored by TLC and

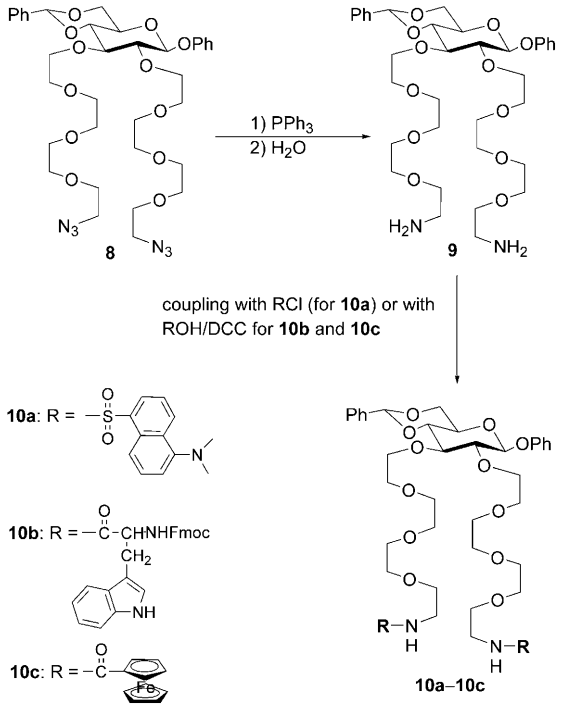

Scheme 3. Synthesis of the labelled glucoside derivatives **10a–10c**.

quenched after the disappearance of the monofunctionalised derivatives, in all cases gave the target compounds in good yields (80–85%).

To test the effective potential of **8** in click chemistry reactions, it was coupled with a suitable terminal alkyne. Here we used substrate **11** (Scheme 4), previously prepared ad hoc by treatment of propargylamine with cholic acid in CH_2Cl_2, in the presence of DCC as the condensing agent. Cholic acid was chosen as a model hydrophobic residue, of interest for the non-covalent immobilisation of biomolecules on hydrophobic surfaces[18] and for the development of novel drug delivery systems,[19] as well as of novel chemosensors for sensitive ion detection.[20] In our hands the reaction was never successful in catalytic mode either with CuI or with the $CuSO_4$/ascorbate system (0.01 up to 0.2 equiv.),

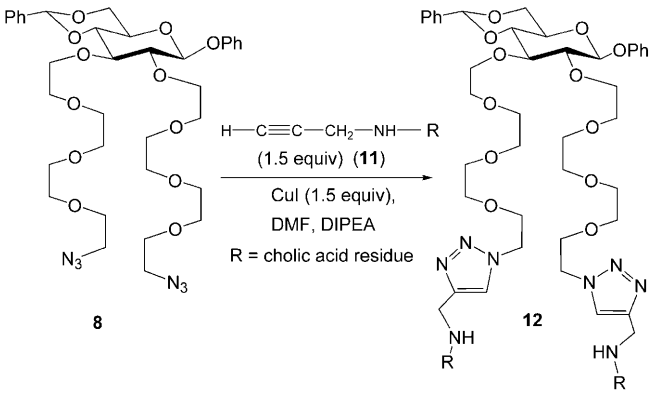

Scheme 4. Synthesis of the labelled glucoside derivative **12**.

even with variation of the solvent and temperature conditions, but good yields of the target compound **12** were finally obtained with addition of CuI in stoichiometric amounts and use of DMF as the solvent in the presence of diisopropylethylamine (DIPEA).

Successive synthetic elaboration of the labelled glucosides **10a–10c** and **12** first involved benzylidene removal, liberating the 6- and 4-OH groups, which exhibited very different reactivities. The obtained compounds might be of interest as such, being amenable to a variety of further manipulations, including immobilisation on a solid support either through direct loading on carboxyl-functionalised resins or through exploitation of derivatisation at C6 through a succinate linker for coupling with an amino-functionalised matrix.[21] Studies directed towards exploitation of these glucoside-functionalised solid supports to generate differently labelled glycoconjugates are in progress. In view of the widely documented use of the dansyl group as an effective probe for mechanistic studies,[11] glucoside **10a** was selected here as a suitable building block to provide the desired environment-sensitive CyPLOS macrocycle.

Synthesis of the dansyl-labelled macrocycle 21: From the starting glucoside **10a**, two building blocks, functionalised as a phosphoramidite (**16**, Scheme 5) and as a 2-chlorophenyl-phosphate derivative, **17**, were prepared, ready for coupling and cyclisation to finally give macrocycle **21**.

In the first step, compound **10a** was converted into the *N*-methyl derivative **13**, to mask the NH groups permanently. Benzylidene removal by standard acidic treatment with diluted trifluoroacetic acid (TFA) in CH_2Cl_2/H_2O gave the 4,6-deprotected derivative **14** in high yields. Treatment with DMTCl (DMT = 4,4′-dimethoxytriphenylmethyl) in pyridine gave almost quantitative yields of the DMT-protected compound **15**, which was then phosphitylated to give the phosphoramidite derivative **16** in 90% yield. The synthesis of the derivative **17** was accomplished in 86% yields over two steps, first involving phosphorylation of the 4-OH group with 2-chlorophenyldichlorophosphate in the presence of triethylamine (TEA) and triazole in pyridine, followed by on-column DMT removal by elution of the silica gel column with $CHCl_3$ with added TFA (0.01%). The coupling of building blocks **16** and **17** was achieved with the aid of 4,5-dicyanoimidazole (DCI) in CH_3CN (0.25 M) as the condensing agent, followed by oxidation with *tert*-BuOOH (5.5 M in decane). The linear dimer **18** (Scheme 6) was isolated after chromatography, involving on-column DMT removal, with 72% yield for the three steps.

The cyclisation of **18** was then carried out by a phosphotriester methodology, with use of 1-mesitylensulfonyl-3-nitro-1,2,4-triazole (MSNT) as the condensing agent under high-dilution conditions ($c \approx 10^{-3}$ M), affording the fully protected **19** in 75% yields. Final deprotection was obtained by treatment first with piperidine, to promote β-elimination of the 2-cyanoethyl protecting group, leading to **20**, and subsequently with a saturated LiOH solution in dioxane/water (1:5, v/v) at 50°C to cleave the 2-chlorophenyl group (95%

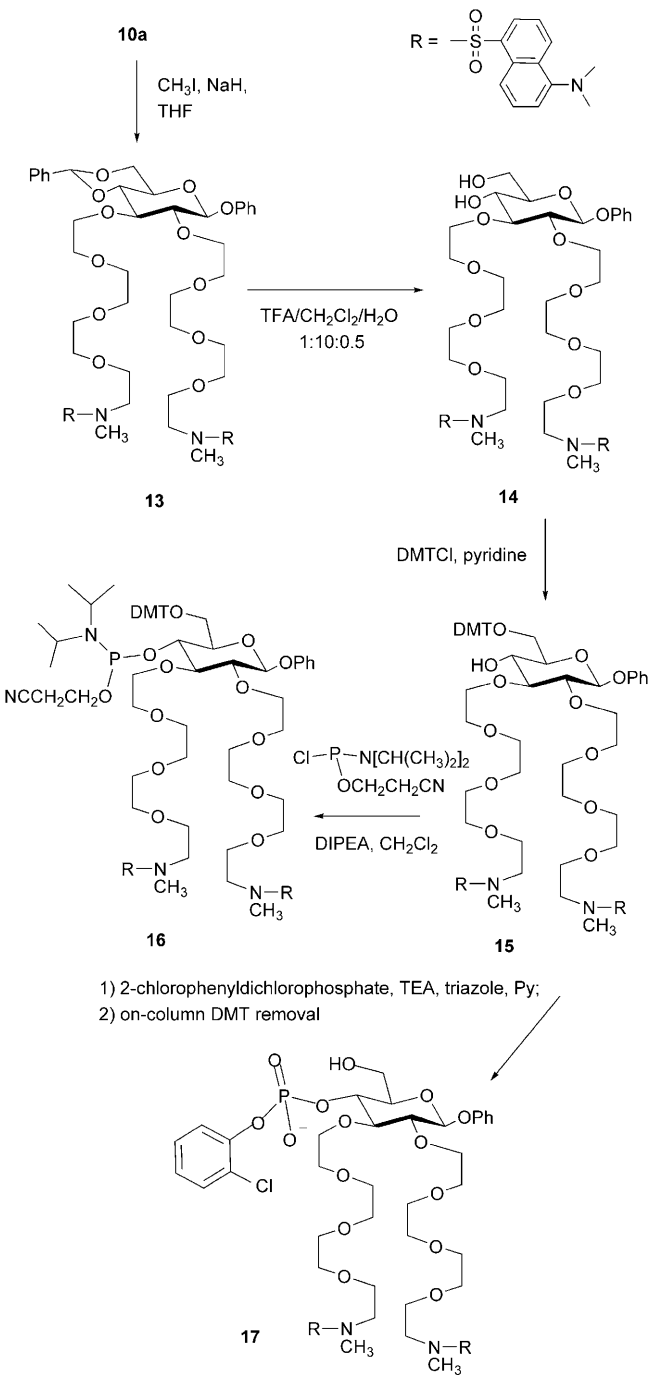

Scheme 5. Synthesis of the labelled building blocks **16** and **17**; Py = pyridine.

yield for the two steps). Compound **21** was prepared by the described procedure in four steps, with 51% yield on average from the building blocks **16** and **17**, each in turn obtained from the glucoside **10a** in four steps with 81–85% yield.

All the intermediates and the final compounds were purified by column chromatography and characterised by ^{1}H and ^{13}C (and ^{31}P, where present) NMR spectrometry and MS analysis

^{31}P NMR spectroscopy studies on the aggregation behaviour of the dansyl-labelled macrocycle 21 in $CDCl_3$: In analogy with the studies previously carried out on the macrocycles **4–6**,[7] compound **21** was analysed by NMR spectroscopy experiments for its tendency to form self-aggregated species in organic solvents. $CDCl_3$, roughly mimicking the polarity of the internal milieu of a lipid bilayer, was the deuterated solvent of choice, offering preliminary, but still useful indications about the behaviour of this amphiphilic macrocycle in bulk membranes. Inspection of the ^{1}H and ^{31}P NMR spectra of **21** showed dramatic line broadening and chemical shift anisotropy of the resonances, diagnostic of slow equilibria on the NMR spectroscopy timescale, which is consistent with the formation of large aggregates in $CDCl_3$.[22] The ^{1}H NMR spectra of **21** did not show any detectable simplification of the spectral lines either with increasing temperature or with increasing dilution of the sample. Concentration-dependent ^{31}P NMR spectroscopic analysis was more informative about the solution behaviour of **21**. At 3.0 mM concentration ($CDCl_3$, 161.98 MHz, 298 K) a very broad signal, centred at about $\delta = 0$ ppm and dispersed over a 15 ppm region, was apparent in its ^{31}P NMR spectrum. Two main bands emerged when the sample was analysed at 1.5 and 0.75 mM, and these then collapsed into a unique large signal centred at about $\delta = 2.0$ ppm when the sample was further diluted to 0.35 mM concentration. At 0.18 mM concentration a well-resolved signal was registered, indicative of the full magnetic equivalence of the two phosphorus atoms in the macrocycle under these conditions. It can be deduced that at this concentration **21** predominantly adopts a symmetric, presumably monomeric and well-solvated form, so that different conformations exist in rapid dynamic equilibria with respect to the NMR spectroscopy timescale. Taken together, these data allowed us to evaluate the critical aggregation concentration (cac) value of **21** over the concentration range of 0.30–0.20 mM (Figure 1). Variable-temperature (VT) ^{31}P NMR spectra for **21** showed no tendency towards even partial simplification of the peaks with increasing temperature up to 338 K, thus indicating the presence of thermally stable aggregates (data not shown). Compound **21** showed a stronger propensity than the previously described benzyl-capped derivative **5** towards self-aggregation in $CDCl_3$, as can be inferred by analysis of their cac values (8–6 mM[7] vs. 0.3–0.2 mM). In part, this can be attributed to possible interactions of the dansyl groups at the extremities of the TEG tails, plausibly contributing to provide extra stabilisation to self-aggregated species through π-stacking interactions.

Characterisation of the aggregates formed by CyPLOS 21 in a pseudo-physiological solution: Self-assembly of amphiphilic ion transporters in physiological solutions, that is, in the aqueous environment surrounding cell membranes, can be crucial for their interactions with the phospholipid bilayers and possibly also for their activity. In principle, nano-aggregation allows these systems to be stabilised in the extracellular media, vehiculated and more easily transferred into the

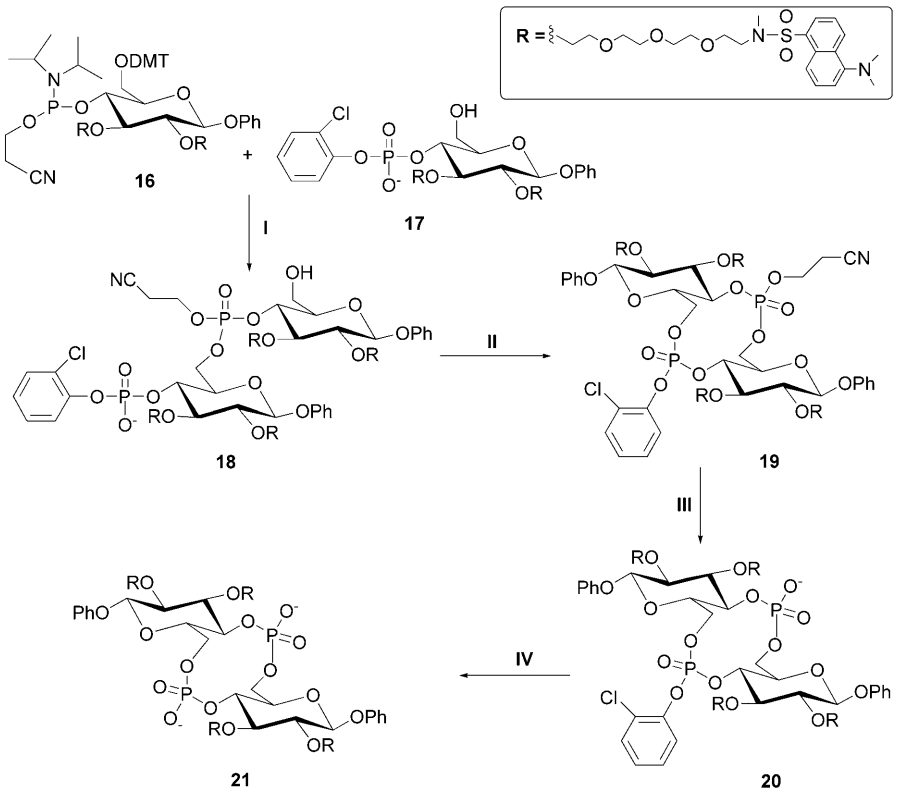

Scheme 6. Synthesis of the macrocycle **21**. i) a) DCI in CH_3CN (0.25 M), RT, 2 h; b) *tert*-BuOOH in decane (5.5 M), RT, 30 min (72% for the two steps); ii) DMAP, MSNT, Py, RT, 12 h (75%); iii) piperidine, 70 °C, 12 h (96%); iv) saturated aq. LiOH/dioxane (5:1, v/v), 50 °C, 12 h (99%).

phospholipid bilayers. From this perspective, we analysed the aggregative behaviour of CyPLOS **21** in a pseudo-physiological solution by means of dynamic light scattering (DLS) and small-angle neutron scattering (SANS) measurements.

Figure 2 shows an example of the diffusion coefficient distribution function obtained at 90° from inverse Laplace transformation of the intensity correlation function $g^{(2)}(t)-1$ for CyPLOS **21** dissolved in a pseudophysiological solution.[23a] Inspection of the figure shows a bimodal distribution with well-separated modes. The slow mode has a greater amplitude than the faster mode, as would be expected for two objects of different sizes diffusing in solution. Provided that the solution is sufficiently dilute, the Stokes–Einstein equation, which rigorously holds at infinite dilution for species diffusing in a continuum medium, may legitimately be used to evaluate the hydrodynamic radius (R_h) of the aggregates [Eq. (1)]:[23b]

$$R_h = \frac{kT}{6\pi\eta D} \qquad (1)$$

in which k is the Boltzmann constant, T is the absolute temperature, and η is the medium viscosity.

Diffusion coefficients, together with hydrodynamic radius values obtained through Eq. (1), are collected in Table 1. The slow diffusive mode found, which corresponds to $R_h = (670 \pm 20)$ nm, is compatible with the presence of large aggregates such as vesicles. On the other hand, the fast diffusive mode is consistent with the presence of smaller aggregates, presumably micelles. The latter have a hydrodynamic radius of 44 nm, which suggests the formation of elongated micelles, probably rod-like aggregates. In fact, the linear length of the molecule, with the assumption of an all-*trans* conformation, is estimated to be around 6 nm, so a hypothetical spherical micelle would have the same radius. On the other hand, the R_h value found for the slow diffusive mode is more than one order of magnitude above the usual size of micellar aggregates, and hence comparable with the size of vesicles. This value is also much higher than the hydrodynamic radii found for the vesicles formed by other CyPLOS molecules. Vesicles formed by **5**, the largest aggregates in the series **4**–**6**, show a value of $R_h = (330 \pm 30)$ nm.[23c] The replacement of benzyl groups with the larger dansyl groups at the ends of the TEG tentacles of CyPLOS backbones therefore seem to affect their overall aggregation behaviour dramatically.

The results obtained by DLS were confirmed by small-angle neutron scattering. Figure 3 reports the scattering cross sections obtained for CyPLOS **21** as a function of the scattering vector modulus q. The cross section profile reveals the presence of large scattering aggregates, typically large vesicles. In particular, the power law $d\Sigma/d\Omega \propto q^{-2}$ is found in the low q region; this trend is typical of bidimensional objects, such as double layers.[23a] A theoretical expression for $d\Sigma/d\Omega$ for a collection of such scattering objects exists[23a] and has been fitted to the experimental data to provide the thickness τ of the double layer. Results of the fitting procedure are reported in Table 1, in which a thickness τ of (13 ± 0.9) nm was obtained. This value is close to double that of the linear extension of the molecule (≈ 6 nm), suggesting a possible conformation not very dissimilar from the all-*trans* disposition and not very pronounced interdigitation between molecules belonging to the two opposite sides of the double layer.

Finally, we would like to highlight the fact that SANS investigations have indeed revealed the presence of vesicles but that it was not possible, unlike in the case of the DLS measurements, to infer the existence of smaller aggregates

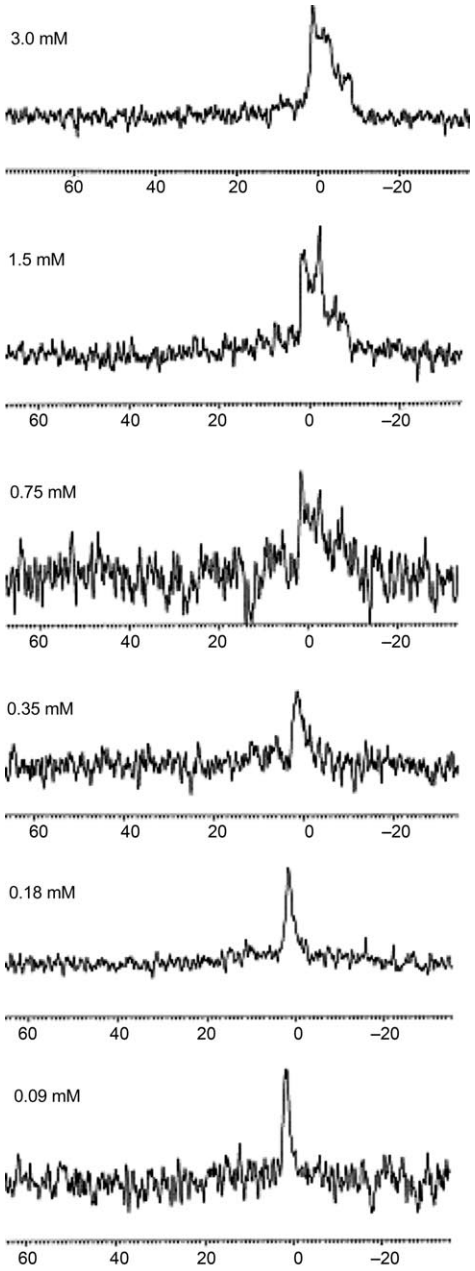

Figure 1. ^{31}P NMR spectra (161.98 MHz, $CDCl_3$, 298 K) of the macrocycle **21** at different concentrations (3.0, 1.5, 0.75, 0.35, 0.18, 0.09 mM).

(micelles). This, of course, does not imply the absolute absence of smaller aggregates, but can be ascribed to an overwhelming predominance of vesicles over micelles in solution, thus rendering the contribution of the smaller aggregates almost negligible. On the other hand, the scattering depends on the square of the volume and consequently is more relevant the larger the aggregates under investigation.

Ionophoric activity of the dansyl-labelled macrocycle 21: In analogy with the previous members of the CyPLOS family, the ionophoric properties of the dansyl-labelled macrocycle **21** were investigated in large unilamellar vesicles (100 nm diameter, prepared by extrusion) with a 95:5 egg phosphatidylcholine (EYPC) and egg phosphatidylglycerol (EYPG) lipid composition. The presence of fluorescent tags in **21** allowed easier determination of the partition coefficient of the ionophore in the membrane than in the case of compound **5**, in which the TEG chains terminate in benzyl groups. The unbound ionophore was separated from the lip-

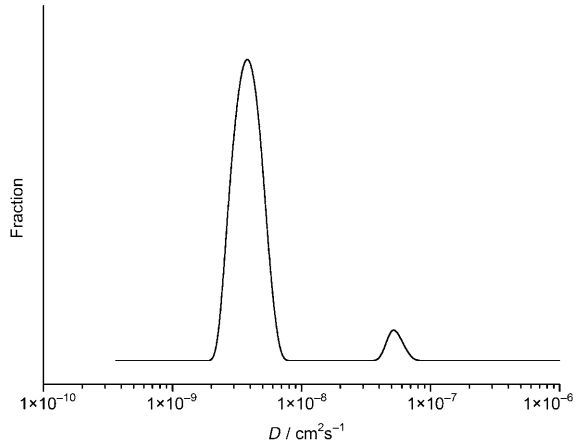

Figure 2. Translational diffusion coefficient distribution function at 25 °C obtained by means of DLS measurements for the binary aqueous system containing CyPLOS **21** at the concentration of 2.00 mmol kg^{-1}.

Table 1. Structural parameters obtained at 25 °C for the aggregates formed by CyPLOS **21** at a concentration of 2.00 mmol kg^{-1}, through DLS and the fitting of the model described in the Experimental section (SANS data). The table reports the translational diffusion coefficients D and hydrodynamic radii R_h for both the diffusive modes, together with the average lamellar thickness τ of vesicular aggregates, determined for the slow diffusive mode.

	D [cm^{2}s^{-1}]	R_h [nm]	τ [nm]
slow mode	**(3.6±0.1)×10^{-9}**	**670±20**	**13.1±0.9**
fast mode	**(5.5±0.3)×10^{-8}**	**44±2**	

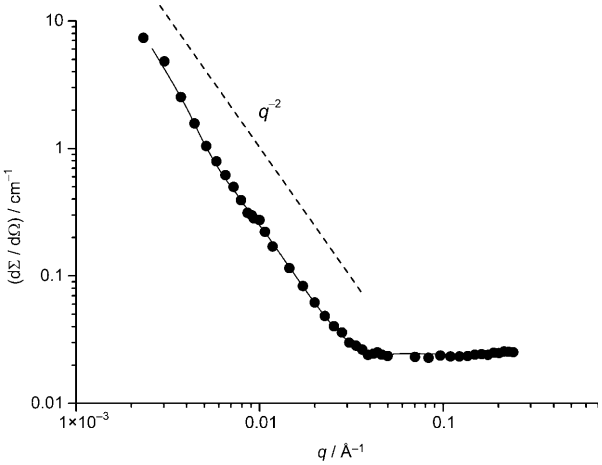

Figure 3. Scattering cross sections obtained at 25 °C by means of SANS measurements for the binary aqueous system containing CyPLOS **21**, at a concentration of 2.00 mmol kg^{-1}. The curve obtained through the fitting of the model described in the experimental part is also shown.

osome suspension with the aid of a gel-permeation column and the liposome fraction, diluted in methanol to destroy aggregated forms, was analysed by fluorescence spectroscopy. Comparison with a calibration curve obtained by measuring the emission intensities of solutions of the ionophore at known concentrations in methanol showed that about 40% of the CyPLOS derivative was partitioned into the membrane.

The ability of the ionophore to mediate a pH gradient collapse across the membrane was measured with the aid of the pH-sensitive fluorescent dye HPTS (HPTS = 8-hydroxypyrene-1,3,6-trisulfonic acid, $pK_a = 7.2$).[24] In this assay the dye is entrapped in phospholipid vesicles buffered at pH 7.0 and, after addition of the ionophore, a pH gradient of 0.6 pH units is applied by external addition of NaOH. The collapse of this transmembrane pH-gradient implies basification of the liposome inner water pool, which is signalled by an increase in the HPTS fluorescence emission. Figure 4a shows the kinetic profiles obtained in the presence of derivative **21** and, for comparison, of CyPLOS **5** both at concentrations of 1%, expressed as the molar ratio of ionophore with respect to total lipid concentration. These data show the dansyl derivative to be a reasonably effective ionophore, with higher activity than compound **5**, which had been the most effective CyPLOS derivative so far tested. Fitting of the data to a first-order rate equation gives the apparent rate constants (k_{obs}, s^{-1}) for the pH-discharge process, which are 4.4×10^{-3} and $1.5\times10^{-3}\,s^{-1}$ for **21** and **5**, respectively. The replacement of the benzyl moieties with the dansyl groups, therefore, roughly doubles the activity of the ionophore.

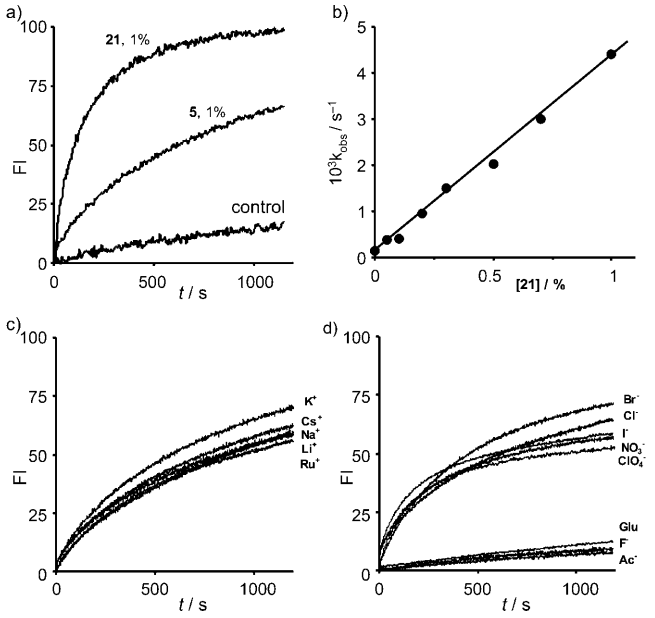

Figure 4. a) Normalised fluorescence change in HPTS emission (FI, λ_{ex} 460 nm, λ_{em} 510 nm) as a function of time after addition of the base (50 μL of 0.5 M NaOH) to 95:5 EYPC/EYPG LUVs (100 nm diameter) loaded with HPTS (0.1 mM HPTS, 0.17 mM total lipid concentration, 25 mM HEPES, 100 mM NaCl, pH 7.0, total volume 3 mL, 25 °C), in the presence of CyPLOS derivatives **21** and **5**. The concentration of the ionophores (1%) is given in percent with respect to the total concentration of lipids. The control trace was recorded in the absence of ionophore. b) Dependence of the apparent rate constants (k_{obs}, s^{-1}) for the pH-discharge process on the % concentration of CyPLOS derivative **21**. c) Cation selectivities for ionophore **21** (0.2% concentration) by HPTS assay (100 mM MCl, pH 7.0, base pulse by addition of 50 μL of 0.5 M MOH). d) Anion selectivities for ionophore **21** (0.2% concentration) by HPTS assay (100 mM NaX, pH 7.0, base pulse by addition of 50 μL of 0.5 M NaOH, Glu = glutamate).

For comparison, the naturally occurring ionophore amphotericin B (AmB), at the same concentration and under the same experimental conditions, is characterised by a $k_{obs} = 2.3\times10^{-3}\,s^{-1}$, which is comparable to the values measured for the CyPLOS derivatives.[8]

The dependence of the apparent rate constant (k_{obs}, s^{-1}) for the pH-discharge process from the concentration of ionophore **21** is shown in Figure 4b. The activity increases linearly with the concentration, suggesting that the active species responsible for the ionophoric process is monomeric. This observation, which parallels the results obtained for compound **5**, is not in contradiction with the aggregation behaviour in low-polarity solvents described above. Indeed, even if account is taken of the partition of the ionophore in the small liposome membrane volume,[25] the concentration used here in the kinetic experiments lies well below the cac determined in $CDCl_3$ (range 0.30–0.20 mM).

The HPTS assay described above can be modified to provide information on the cation/anion selectivity of the transport process.[24] Indeed, the basification of the inner water pool as a response to the pH gradient has to be balanced to maintain the ionic strength constant. The basification may originate either from H^+ efflux or from OH^- influx and so four overall transmembrane charge translocation transport processes can be set up to balance the pH increase: H^+/Na^+ antiport, OH^-/Cl^- antiport, H^+/Cl^- symport and Na^+/OH^- symport. In this modified version of the HTPS assay the liposome suspension is prepared in a HEPES buffer (pH 7.0) containing 100 mM MCl or NaX (in which M and X are the cation and anion under investigation, respectively) and the pH gradient is established with NaOH in the cation selectivity experiments or MOH in the anion selectivity experiments. The observed HPTS fluorescence emission changes therefore report indirectly on the effect of the cation/anion present on the overall transport process. The results obtained are reported in Figure 4c and d for the cation and anion selectivity experiments, respectively. The activity is not significantly affected with a change in the Group I alkali metal cation present (Figure 4c). On the other hand, the anions show a strong effect on the transport process (Figure 4d) and they group into two distinct families: the more hydrophilic ones (fluoride, acetate, glutamate), which are almost not transported, and the less hydrophilic ones (the other halogens, nitrate and perchlorate) which are efficiently transported, but all at a similar rate. This behaviour (indifference to the cation present and anion-hydrophilicity-controlled off/on behaviour in the transport of the anions) strictly parallels that described for compound **5**, which has been interpreted in terms of a transport process dominated

by OH^-/X^- antiport or H^+/X^- symport in which the rate-limiting factor switches from X^- to H^+ (or OH^-) transport with decreasing anion hydration energy.[8] Highly hydrophilic anions are not transported, but when the dehydration cost decreases below that of acetate, the process is controlled by H^+ (or OH^-) transport, and all the anions with lower hydration energy are therefore transported at a similar rate. In any case the absence of selectivity among the transported anions suggests the formation of a poorly structured pore and little or no interaction between the transported species and the ionophore. However, control experiments with the relatively large calcein dye indicate that the pore formed, whatever its structure, is not large enough to allow the transport of calcein and that the ionophore is not able to cause lysis of the liposomes, at least up to the highest concentration tested (7%, in terms of ionophore/phospholipids ratio).

The emission spectra of the dansyl dye exhibit large solvent-dependent fluorescent shifts and this property might provide valuable information on its position when inserted in a phospholipid bilayer.[11] The fluorescence spectra of the dansyl-labelled macrocycle **21** (1.7 μM) were recorded in solvents of different polarities and the observed emissions (λ_{max}) were plotted against Reichardt's E_T polarity parameter (Figure 5).[26] Fitting of the data gives a linear correlation ($y=1.1x+458.87$, $r^2=0.9807$) over the range of the solvents

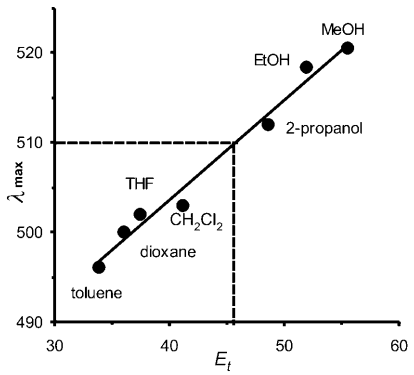

Figure 5. Plot of fluorescence emission maxima for **21** ([**21**]=1.7 μm) in solvents of different polarity. The dotted lines correspond to emission maxima of **21** ([**21**]=3.4 μm, λ_{ex}=340 nm) measured in an EYPC/EYPG suspension (95:5, [total lipid]=0.17 mM, 25 mM HEPES, 100 mM NaCl, pH 7.0).

investigated. Similar linear correlations were also obtained with different polarity scales, such as Z, or by plotting the λ_{max} values against the dielectric constants (ε) of the solvents. However, the solvent polarity parameter E_T is determined directly by spectral measurements in solution and so its use appears more appropriate in the present case.[11a]

The fluorescence maximum for **21** in EYPC/EYPG liposomes (95:5, [**21**]=3.4 μM, [total lipid]=0.17 mM) was 509 nm. This corresponds to an E_T value of 45.5, intermediate between the alcohols and the less polar solvents. Because the phospholipid bilayer can be thought of as having four polarity regimes[11d], 1) the surface (water polarity), 2) the phosphoryl headgroup (high polarity), 3) the glyceryl esters (mid-polar regime, medium polarity) and 4) the insulator regime (hydrocarbon-like polarity), the observed value suggests that the dansyl groups of **21** are located at or near the mid-polar (glyceryl) region of the bilayer. This observation is consistent with the mode of insertion in the membrane postulated for the previously investigated CyPLOS derivatives.[8] The polar, negatively charged, macrocycle lies on the surface of the membrane with the four amphiphilic TEG chains inserted in the phospholipid bilayer. The TEG chains are apparently not deeply inserted in the phospholipid bilayer but are located in the midpolar region in-between the polar surface and the hydrocarbon core of the membrane. This, probably, results in a destabilisation of the structure of the membrane and, therefore, in alteration of its permeability. Taken together, the data obtained for compound **21** confirm the general picture on the mechanism of action that was drawn for CyPLOS **5**, experimentally supporting its mode of insertion in the membranes. The higher activity observed for **21** could probably be related either to greater partition of the more lipophilic derivative in the membrane, or to the larger size of the dansyl residues relative to the benzyl groups, which may result in a more effective perturbation of the phospholipid bilayer order.

Interestingly, the fluorescence maximum (λ_{max}) observed for **21** (3.4 μM) in HEPES buffer was 496 nm. Interpolation results in an E_T value of 34, lower that that obtained when the ionophore is inserted in the membrane. This result indicates that the dansyl dye is experiencing a less polar environment in an aqueous buffer, suggesting the formation of pre-aggregates in water even at this very low concentration. Apparently, these pre-aggregates are destroyed when the CyPLOS derivative partitions in the membrane, as suggested by the kinetic profile of Figure 4b and by the change in the emission spectra of the dansyl group.

Conclusion

A novel, dansyl-labelled CyPLOS analogue, **21**, is described and synthesised in 12 steps and 26% overall yield from the starting benzylidene-protected phenyl β-D-glucopyranoside **7**. The overall strategy is based on the synthesis of a versatile glucoside containing azido functionalities, **8**, which—through straightforward and high-fidelity reactions—gave easy access to differently labelled monosaccharides (**10a**–**10c** and **12**), prepared here as model synthetic scaffolds. These multifunctional entities are of potential interest themselves in a diversity-oriented synthetic approach for the preparation of various glycoconjugates or glyco-architectures, tailored for the development of sophisticated sensors in biomolecule detection and in supramolecular chemistry. In this context, these glucosides might be exploitable as useful precursors to provide diversely functionalised CyPLOS analogues.

Synthetic elaboration of the dansyl-labelled glucoside **10a** gave the phosphorylated building blocks **16** and **17**, which, after coupling, cyclisation and final deprotection, furnished the target macrocycle **21**. The self-assembly properties of this molecule in $CDCl_3$ and in a pseudo-physiological aqueous solution were studied, and it was shown to form stable aggregated systems in both media. Concentration-dependent ^{31}P NMR spectroscopic analysis allowed a critical aggregation concentration in the 0.3–0.2 mM range to be estimated for this amphiphilic macrocycle in $CDCl_3$, which is an environment roughly mimicking the polarity of the mid-polar region of the phospholipid bilayers. Characterisation of the aggregative behaviour of **21** in aqueous solution, providing useful information on its organisation prior to membrane insertion, was carried out by a combined experimental approach, using DLS measurements to reveal the formation and size distribution of the aggregates and SANS measurements to give an estimation of the thickness of the aggregates. The data obtained from DLS and SANS studies showed that in an aqueous environment **21** is mainly organised in the form of large vesicles, much greater in size than all previously investigated CyPLOS molecules. DLS data also revealed the presence in a pseudo-physiological buffer of smaller aggregates, presumably micelles, and the diffusion coefficients and the hydrodynamic radii for both systems were determined.

The HPTS assay showed **21** to be able to discharge a pH gradient across a liposomal membrane completely in 15 min at 1% ionophore concentration, therefore displaying a higher activity than all the CyPLOS derivatives described previously, although the determination of the cation and anion selectivities and of other kinetic parameters suggests a common mechanism of action. The presence of the dansyl dye gave valuable information on the mode of insertion of the ionophore in the membrane, essentially confirming the overall mechanism of action previously hypothesised for its analogues. In particular, in EYPC/EYPG liposomes at the concentration used in the kinetic experiments, the ionophore appears to be active in a monomeric form with the polar macrocyclic head lying on the surface of the membrane and the four amphiphilic TEG chains inserted in the phospholipid bilayer. The TEG chains are apparently not deeply inserted in the phospholipid bilayer but are located in the mid-polar region in-between the polar surface and the hydrocarbon core of the membrane. This probably results in a destabilisation of the structure of the membrane and therefore in the alteration of its permeability.

At 1% ionophore concentration, aggregation processes for **21** may be considered—at least to a first approximation—negligible within the phospholipid bilayers, and the ionophoric activity may therefore be reasonably accounted for by simple monomeric forms, which can generate defects capable of facilitating ion trafficking. On the other hand, in an aqueous milieu, this amphiphilic ion transporter has a strong tendency to form stable self-assembled systems even at μM concentrations, as also confirmed by the fluorescence shift of the appended dansyl dye. Such high levels of pre-aggregation, allowing these systems to be vehiculated and stabilised in the extracellular media, and eventually transferred into the phospholipid bilayers, can be crucial for their dynamic interactions with cell membranes and their activity. Future studies will be addressed at the specific investigation of these aspects, so as to produce ionophores with increased activity and selectivity. For this purpose, novel differently end-functionalised CyPLOS derivatives will be produced, with advantage taken of the ready synthetic access to diverse analogues in this class of molecules and also with exploitation of the major role played by the reporter groups attached to their tentacles both in aggregation and in ion-transport activity.

Experimental Section

General methods: All reagents were of the highest commercially available quality and were used as received. TLC analyses were carried out with silica gel plates (Merck, 60, F254). Reaction products on TLC plates were visualised with UV light and then by treatment with a $Ce(SO_4)_2$/H_2SO_4 aqueous solution (10%). For column chromatography, silica gel (Merck Kieselgel 40, 0.063–0.200 mm) was used. The following abbreviations are used throughout the text: AcOEt = ethyl acetate; Dans = dansyl (that is, 5-*N*,*N*-dimethylaminonaphthalenesulfonyl); DBU = 1,8-diazabicyclo[5,4,0]undec-7-ene; DCC = dicyclohexylcarbodiimide; DCI = 4,5-dicyanoimidazole; DIPEA = *N*,*N*-diisopropylethylamine; DMAP = 4-(*N*,*N*-dimethylamino)pyridine; DMF = *N*,*N*-dimethylformamide; DMT = 4,4′-dimethoxytriphenylmethyl; EtOH = ethanol; AcOEt = ethyl acetate; Fmoc = 9-fluorenylmethoxycarbonyl; HOBt = 1-hydroxybenzotriazole; HPTS = 8-hydroxypyrene-1,3,6-trisulfonic acid, trisodium salt; MSNT = 1-mesitylensulfonyl-3-nitro-1,2,4-triazole; Ph_3P = triphenylphosphine; TEG = tetraethylene glycol; THF = tetrahydrofuran; TEA = triethylamine; TFA = trifluoroacetic acid.

NMR spectra were recorded with Bruker WM 400, Varian Gemini 300, Varian Gemini 200 and Varian Inova 500 spectrometers as specified, in all cases at 25 °C. All the chemical shifts are expressed in ppm with respect to the residual solvent signal. Peak assignments were carried out through standard H–H COSY and HSQC experiments. For the ESI MS analyses, a Waters Micromass ZQ instrument—fitted with an Electrospray source—was used in the positive and/or negative mode. MALDI TOF mass spectrometric analyses were performed with a PerSeptive Biosystems Voyager-De Pro MALDI mass spectrometer in the Linear mode with 3,4-dihydroxybenzoic acid as the matrix.

Preparation of the investigated systems: All the samples used for DLS and SANS investigations were prepared by direct weighing of all the components. In particular, for each solution an appropriate amount of the solute was dissolved in an appropriate buffer solution at pH 7.4, in order to provide a final concentration of 2.00 mmol kg^{-1}. Because of the intrinsically slow kinetics, dissolution was promoted by slight warming (≈40 °C) and a short sonication treatment (≈15 min).

The buffer solution was obtained by starting from an aqueous solution of NaCl (0.140 mol dm^{-3}) and KH_2PO_4 (0.010 mol dm^{-3}), prepared in distilled and previously degassed water, and by adding an appropriate amount of KOH up to pH 7.4. This value was checked to be within 0.1 pH units with a Radiometer pHM220 pH-meter, with a saturated calomel electrode and a glass electrode previously calibrated with the IUPAC standard buffer solutions.[24] For SANS measurements, heavy water (D_2O, isotopic enrichment > 99.8%, molar mass 20.03 g mol^{-1}), purchased from Aldrich and used as such, was used as the solvent in order to minimise the incoherent contribution to the scattering cross sections arising from the system.

SANS measurements: Small-angle neutron scattering measurements were performed at 25 °C with the KWS2 instrument located at the Heinz

Maier-Leibnitz neutron source of the Jülich Centre for Neutron Science (Garching, Germany). Neutrons with an average wavelength of 7 Å and 19 Å and a wavelength spread $\Delta\lambda/\lambda \leq 0.2$ were used. A two-dimensional 128×128 array scintillation detector at two different collimation (C)/sample-to-detector(D) distances (C_8D_8 and C_8D_2, with all the lengths express in m) measured neutrons scattered from the samples. These configurations allowed data collection in a range of the scattering vector modulus $q=4\pi/\lambda\sin(\theta/2)$ located between 0.002 and 0.33 $Å^{-1}$, with θ scattering angle. The obtained raw data were then corrected for background and empty cell scattering. Detector efficiency corrections, radial average and transformation to absolute scattering cross sections $d\Sigma/d\Omega$ were made with a secondary plexiglass standard.[28,29]

DLS measurements: Dynamic light scattering investigations were performed with a setup composed of a Photocor compact goniometer, a SMD 6000 Laser Quantum 50 mW light source operating at 5325 Å and a PMT and correlator obtained from Correlator.com. All the measurements were performed at (25.00 ± 0.05) °C with use of a thermostat bath.

In DLS, the intensity autocorrelation function $g^{(2)}(t)$ is measured and related to the electric field autocorrelation $g^{(1)}(t)$ by the Siegert relation.[30] $g^{(1)}(t)$ can in turn be related, through a Laplace transform, to the distribution function of the relaxation rates Γ from which the z-average of the diffusion coefficient D may be obtained [Eq. (2)]:[31]

$$D=\lim_{q\to0}\frac{\Gamma}{q^2} \tag{2}$$

in which $q=4\pi n_0/\lambda\sin(\theta/2)$ is the modulus of the scattering vector, n_0 is the refractive index of the solution, λ is the incident wavelength, and θ represents the scattering angle. D is thus obtained from the limit slope of Γ as a function of q^2, in which Γ is measured at different scattering angles.

Ionophoric activity

General procedures: L-α-Phosphatidyl-DL-glycerol sodium salt (EYPG, 20 mg mL^{-1} chloroform solution) was purchased from Avanti Polar Lipids; egg yolk phosphatidylcholine (EYPC, 100 mg mL^{-1} chloroform solution) and 8-hydroxypyrene-1,3,6-trisulfonic acid trisodium salt (HPTS) were from Sigma. Triton X-100 and HEPES buffer were from Fluka; all salts were of the best grade available from Aldrich and were used without further purification.

Ultrafiltration was performed with Microcon YM-10 filters from Millipore. Size exclusion chromatography (SEC) was performed with Sephadex G-75 or pre-packed columns Sephadex G-25 M (PD-10) from Amersham Biosciences.

Liposomes were prepared by extrusion with use of a Lipex Thermobarrel EXTRUDER (10 mL, Northern Lipids. Inc.) connected to a thermostatic bath (25 °C if not otherwise indicated). The 100 nm polycarbonate membranes are Nucleopore Track-Etch Membranes from Whatman.

Fluorescence spectra were recorded with a Perkin–Elmer LS-50B fluorimeter and a Varian Cary Eclipse Fluorescence spectrophotometer. UV spectra were recorded with a Unicam helios β UV/Vis spectrophotometer. For solvent-dependence experiments, freshly distilled solvent (2 mL) was used instead of buffer.

The concentrations of ionophores are given as percentages with respect to the total concentrations of lipids. Mother solutions of ionophores were prepared in DMSO. Control experiments showed that the amounts of DMSO added to the vesicular suspensions in the different experiments (maximum amount 1.0% in volume) did not affect the permeabilities of the membranes.

HPTS assay: A mixture of EYPC chloroform solution (100 mg mL^{-1}, 225 μL, 30 μmol) and EYPG chloroform solution (20 mg mL^{-1}, 60 μL, 1.5 μmol) was first concentrated under an Ar flow to form a thin film and then dried under high vacuum for 3 h. The lipid cake was hydrated in HPTS solution (HEPES (25 mM), NaCl (100 mM), pH 7, 1.5 mL, 0.1 mM) for 30 min at 40 °C. The lipid suspension was subjected to five freeze-thaw cycles (−196 °C/40 °C) with use of liquid nitrogen and a thermostatic bath, and then extruded under nitrogen pressure (15 bar) at room temperature (10 extrusions through a 0.1 μm polycarbonate membrane). The LUV suspension was separated from extravesicular dye by size exclusion chromatography (SEC) (stationary phase: pre-packed column Sephadex G-25, mobile phase: HEPES buffer) and diluted with HEPES buffer to give a stock solution with a lipid concentration of 5 mM (with the assumption that 100% of lipids were incorporated into liposomes). The lipid suspension (104 μL) was placed in a fluorimetric cell, diluted to 3040 μL with the same buffer solution as used for the liposome preparation and kept with gentle stirring. The total lipid concentration in the fluorimetric cell was 0.17 mM. An aliquot of solution of the ionophore (5–30 μL of the appropriate mother solution in order to obtain the desired $mol_{compound}/mol_{lipid}$ ratio) was then added to the lipid suspension and the cell was incubated at 25 °C for 30 min. After incubation the time course of fluorescence was recorded for 200 s (λ_{ex} 460 nm, λ_{em} 510 nm), NaOH (0.5 M, 50 μL) was then rapidly added through an injector port, and the fluorescence emission was recorded for 1200 s. Maximum changes in dye emission were obtained by final lysis of the liposomes with detergent (40 μL of 5% aqueous Triton X-100). Fluorescence time courses were normalised by use of the following equation [Eq. (3)]:

$$FI=\frac{(F^t-F^0)}{(F^\infty-F^0)}\times100 \tag{3}$$

where F^t is the fluorescence intensity measured at time t, F^0 is the fluorescence intensity at ionophore addition, and F^∞ is the fluorescence intensity at saturation after lysis with Triton. The apparent first-order rate constants for the transport process were obtained by nonlinear regression analysis of the fluorescence data vs. time.

Determination of cation and anion selectivity by HPTS assay: The vesicle suspension (104 μL stock solution, prepared as described above) was placed in a fluorimetric cell and diluted to 3040 μL with the appropriate buffer solution (HEPES (pH 7, 25 mM), MCl (100 mM) with $M=Li^+$, Na^+, K^+, Rb^+, Cs^+, or NaX (100 mM) with $X=F^-$, Cl^-, Br^-, I^-, NO_3^-, ClO_4^-, Ac^-, Glu). The total lipid concentration in the fluorimetric cell was 0.17 mM. An aliquot of DMSO solution of the ionophore (5–30 μL of the appropriate mother solution in order to obtain the desired $mol_{compound}/mol_{lipid}$ ratio) was then added to the lipid suspension and the cell was incubated at 25 °C for 30 min. After incubation the time course of fluorescence was recorded for 200 s (λ_{ex} 460 nm, λ_{em} 510 nm) and then MOH (0.5 M, with $M=Li^+$, Na^+, K^+, Rb^+, Cs^+ depending on the cation present in the extravesicular buffer solution, 50 μL) was rapidly added through an injector port and the fluorescence emission was recorded for 1200 s. Maximum changes in dye emission were obtained by final lysis of the liposomes with detergent (aqueous solution of Triton X-100, 5%, 40 μL). Fluorescence time courses were normalised as previously described.

Calcein release assay: The LUV suspension was prepared as previously described with a mixture of EYPC chloroform solution (100 mg mL^{-1}, 9.5 μmol, 72 μL) and EYPG chloroform solution (20 mg mL^{-1}, 0.5 μmol, 19 μL). The lipid cake was hydrated in calcein solution (HEPES (pH 7.4, 1 mM) 50 mM, 2.0 mL). The LUV suspension was separated from extravesicular dye by size exclusion chromatography (SEC, stationary phase: column Ø1 × 25 cm Sephadex G-75, mobile phase: buffer HEPES (1 mM), NaCl (150 mM), pH 7.4) and diluted with the same HEPES buffer to give a stock solution with a final lipid concentration of 0.4 mM (with the assumption that 100% of lipid was incorporated into liposomes). The vesicle suspension (550 μL stock solution) was placed in a fluorimetric cell and diluted to 2200 μL with the buffer solution used for preparation. The total lipid concentration in the fluorimetric cell was 0.1 mM. Calcein emission was monitored at 520 nm with excitation at 490 nm. During the experiment, aliquots of DMSO solution of the ionophore were then added up to the maximum concentration investigated, of 7% ionophore. Maximum changes in dye emission were obtained by lysis of liposomes with detergent (aqueous Triton X-100 solution, 5%, 40 μL).

Ionophore partition in liposome: The vesicle suspension was prepared as described above in HEPES buffer (25 mM), NaCl (100 mM), pH 7, with a final total concentration of lipids of 3.7×10^{-3} M. An aliquot of mother solution of compound **21** was added in order to obtain a 1% concentration of ionophore. After 30 min of incubation at 25 °C, the LUV suspension

was separated from non-membrane-bound **21** by size exclusion chromatography (SEC, stationary phase: pre-packed column Sephadex G-25, mobile phase: HEPES buffer). The liposome fraction eluted from the column was analysed for the ionophore content: an aliquot of the suspension was dissolved in methanol and the fluorescence emission of the dansyl dye was measured ($\lambda_{ex}=340$ nm). The maximum of emission intensity ($\lambda_{em}=520$ nm) was correlated to the ionophore concentration with the aid of a calibration curve obtained by measuring the emission intensities of solutions of ionophore at known concentrations in methanol.

Synthesis of TEG-azido III

Synthesis of I: Ag_2O (1.1 g, 4.7 mmol) and *p*-toluenesulfonyl chloride (1.0 g, 5.2 mmol) were sequentially added to a solution of tetraethylene glycol (0.89 g, 4.6 mmol) in anhydrous CH_2Cl_2 (10 mL). The reaction mixture was stirred at room temperature for 48 h. The reaction mixture was filtered on celite and washed twice with AcOEt and then with a saturated NaCl solution. The organic phase, dried over anhydrous Na_2SO_4, was filtered, concentrated under reduced pressure and then chromatographed on a silica gel column. Elution with $CHCl_3$ containing increasing amounts of CH_3OH (from 0 to 5%) gave the product **I** (1.3 g, 3.7 mmol) in 80% yield. Oil, $R_f=0.35$ ($CHCl_3/CH_3OH$ 95:5, v/v); ^{1}H NMR (500 MHz, $CDCl_3$): $\delta=7.81$–7.33 (m, 4H; aromatic protons), 4.16 (t, ^3J(H,H)=4.8, 4.8 Hz, 2H; -CH_2-SO_2), 3.72–3.60 (overlapped signals, 14H; 7×-O-CH_2-*TEG*), 2.44 ppm (s, 3H; −CH_3); ^{13}C NMR (125 MHz, $CDCl_3$): $\delta=144.7$, 129.7, 127.9 and 104.2 (aromatic carbons), 72.4, 70.7, 70.6 70.4, 70.2, 69.1, 68.6 and 61.7 (-O-CH_2-*TEG*), 21.5 ppm (−CH_3); MS (ESI$^+$): *m/z*: calcd for $C_{15}H_{24}O_7S$: 348.1243; found: 371.23 $[M+Na]^+$, 387.20 $[M+K]^+$.

Synthesis of II: NaN_3 (721 mg, 11.1 mmol) was added to a solution of **I** (1.3 g, 3.7 mmol), dissolved in anhydrous EtOH (15 mL). The solution was stirred for 8 h at reflux and then concentrated under reduced pressure. The reaction mixture, diluted in $CHCl_3$, was washed twice with a saturated NaCl solution. The organic phase, dried over anhydrous Na_2SO_4, was filtered and concentrated under reduced pressure to give **II** (0.81 g, 3.7 mmol), which was used as such without further purification. Oil, $R_f=0.30$ ($CHCl_3/CH_3OH$ 95:5, v/v); ^{1}H NMR (500 MHz, $CDCl_3$): $\delta=3.71$–3.59 (overlapped signals, 12H; 6×-O-CH_2-*TEG*), 3.41 (t, 2H; -CH_2-OH), 2.32 ppm (t, 2H; -CH_2-N_3); ^{13}C NMR (125 MHz, $CDCl_3$): $\delta=72.3$, 70.5, 70.2, 69.9 (-O-CH_2-*TEG*), 61.6 (-CH_2-OH), 50.5 ppm (−CH_2N_3); MS (ESI$^+$): *m/z*: calcd for $C_8H_{17}N_3O_4$: 219.1219; found: 242.22 $[M+Na]^+$, 258.21 $[M+K]^+$.

Synthesis of III: DIPEA (1.5 mL, 8.6 mmol) and methanesulfonyl chloride (345 μL, 4.4 mmol) were sequentially added to compound **II** (0.81 g, 3.7 mmol), dissolved in anhydrous CH_2Cl_2 (8 mL), and the resulting mixture was left overnight at room temperature. The reaction mixture was then concentrated under reduced pressure, transferred into a separating funnel and washed twice with a saturated NaCl solution. The organic phase, dried over anhydrous Na_2SO_4, was filtered, concentrated under reduced pressure and then chromatographed on a silica gel column. Elution with $CHCl_3$ gave product **III** (0.99 g, 3.4 mmol) in 92% yield. Oil, $R_f=0.6$ ($CHCl_3/CH_3OH$ 95:5, v/v); MS (ESI$^+$): *m/z*: calcd for $C_9H_{19}N_3O_6S$: 297.0995; found: 320.19 $[M+Na]^+$, 336.28 $[M+K]^+$.

Synthesis of 8: Compound **7** (380 mg, 1.1 mmol), prepared as previously described,[6] was dissolved in anhydrous DMF (7.0 mL) and treated with sodium hydride (80 mg, 3.4 mmol). The mixture was stirred for 10 min, and compound **III** (0.99 g, 3.4 mmol) was then added at room temperature. After 4 h with stirring, the reaction mixture was quenched by addition of CH_3OH and concentrated under reduced pressure. The crude product was then diluted with $CHCl_3$, transferred into a separating funnel and washed three times with water. The organic phase was concentrated under reduced pressure and purified by column chromatography. Elution of the column with $CHCl_3$ containing increasing amounts of CH_3OH (from 0% to 5%) gave product **8** (665 mg, 0.90 mmol) in 82% yield. Oil, $R_f=0.35$ ($CHCl_3/CH_3OH$ 95:5, v/v); ^{1}H NMR (400 MHz, $CDCl_3$): $\delta=7.46$–7.01 (complex signals, 10H; aromatic protons), 5.52 (s, 1H; Ph−C*H*), 5.01 (d, ^3J(H,H)=7.6 Hz, 1H; H-1), 4.33 (m, 1H; H-4), 4.05–3.88 (overlapped signals, 5H; -CH_2-O-C-2, -CH_2-O-C-3 and H-6_a], 3.76 (t, $J=10.4$, 10.0 Hz, 1H; H-3), 3.64–3.57 (overlapped signals, 25H; 12×O-CH_2-*TEG* and H-6_b), 3.51–3.43 (overlapped signals, 2H; H-2 and H-5), 3.34 ppm (t, ^3J(H,H)=4.8, 4.8 Hz, 4H; -CH_2-N_3); ^{13}C NMR (75 MHz, $CDCl_3$): $\delta=156.9$, 137.0, 129.5, 129.3, 128.8, 128.0, 125.9, 122.8, 116.8 and 116.3 (aromatic carbons), 101.6 (C-1), 101.0 (Ph−*C*H), 82.3 (C-2), 81.5 and 80.4 (2×-CH_2-CH_2-O-sugar), 77.1 (2×-CH_2-CH_2-N_3), 72.4 and 72.2 (2×-CH_2-O-sugar), 70.4 (12×O-CH_2 *TEG*), 70.2 (C-6), 69.8 (C-3), 68.5 (C-4), 66.0 (C-5), 50.4 ppm (2×-CH_2-N_3); IR (KBr): $\tilde{\nu}_{max}=2104$, 1636, 1558, 1490, 1456, 1225, 1085, 1036, 771, 706 cm^{-1}; MS (MALDI$^+$): *m/z*: calcd for $C_{35}H_{50}N_6O_{12}$: 746.3487; found: 747.49 $[M+H]^+$, 769.59 $[M+Na]^+$, 785.62 $[M+K]^+$; HRMS (MALDI-TOF): *m/z*: calcd for $C_{35}H_{50}N_6O_{12}Na$: 769.3384; found: 769.3398 $[M+Na]^+$.

Synthesis of 9: Compound **8** (320 mg, 0.43 mmol) was dissolved in anhydrous THF (2 mL), Ph_3P (281 mg, 2.5 mmol) was then added, and the solution was stirred at room temperature for 8 h. Next, water was added (5 mL) and the resulting mixture was left stirring for 48 h. The reaction mixture was treated with a dilute aqueous HCl solution and then washed several times with diethyl ether to remove the impurities. The aqueous phase was then neutralised and extracted with $CHCl_3/CH_3OH$ (9:1, v/v), and the organic phases were collected and taken to dryness, giving pure **9** (300 mg, 0.43 mmol, almost quantitative yields), which was used as such without further purification. Oil, $R_f=0.4$ (*n*-butanol/acetic acid/water 60:15:25, v/v/v); ^{1}H NMR (500 MHz, $CDCl_3$): $\delta=7.48$–7.02 (complex signals, 10H; aromatic protons), 5.53 (s, 1H; Ph−C*H*), 5.02 (d, ^3J(H,H)=8.0 Hz, 1H; H-1), 4.34 (m, 1H; H-4), 4.07–3.89 (overlapped signals, 4H; -CH_2-O-C-2 and -CH_2-O-C-3), 3.77 (t, ^3J(H,H)=10.0 and 10.5 Hz, 1H; H-3), 3.65–3.52 (overlapped signals, 27H; 12×(O-CH_2-*TEG*), H-2 and H_2-6), 3.47 (m, 1H; H-5), 2.83 ppm (brs, 4H; 2×-CH_2-NH_2); ^{13}C NMR (125 MHz, $CDCl_3$): $\delta=157.0$, 137.1, 132.0, 129.4, 128.9, 128.3, 128.1, 125.9, 122.8 and 116.9 (aromatic carbons), 101.7 (C-1), 101.1 (Ph−*C*H), 82.4 (C-2), 81.5 and 80.5 (2×-CH_2-CH_2-O-sugar), 73.3 (2×-CH_2-CH_2-NH_2), 72.4 and 72.2 (2×-CH_2-O-sugar), 70.6, 70.5, 70.4 and 70.3 (12×O-CH_2 *TEG*), 70.2 (C-6), 70.1 (C-3), 68.5 (C-4), 66.0 (C-5), 41.6 ppm (2×CH_2-NH_2); IR (KBr): $\tilde{\nu}_{max}=3504$ (broad), 1638, 1558, 1486, 1452, 1230, 1089, 1032, 772, 699 cm^{-1}; MS (MALDI$^+$): *m/z*: calcd for $C_{35}H_{54}N_2O_{12}$: 694.3677; found: 695.93 $[M+H]^+$, 717.95 $[M+Na]^+$, 733.83 $[M+K]^+$; HRMS (MALDI-TOF): *m/z*: calcd for $C_{35}H_{54}N_2O_{12}Na$: 717.3574; found: 717.3583 $[M+Na]^+$.

Synthesis of dansyl-tagged derivative 10a: Compound **9** (130 mg, 0.19 mmol), previously dried by repeated coevaporations with anhydrous benzene and kept under reduced pressure, was dissolved in anhydrous CH_2Cl_2 (3 mL). TEA (100 μL, 0.76 mmol) and dansyl chloride (150 mg, 0.57 mmol) were sequentially added and the resulting mixture was left stirring overnight at room temperature. The reaction mixture was then concentrated under reduced pressure, transferred into a separating funnel and washed twice with a saturated NaCl solution. The organic phase, dried over anhydrous Na_2SO_4, was filtered, concentrated under reduced pressure and then chromatographed on a silica gel column. Elution with $CHCl_3$ containing increasing amounts of CH_3OH (from 0% to 5%) gave product **10a** (185 mg, 0.16 mmol) in 85% yield. Oil, $R_f=0.5$ ($CHCl_3/CH_3OH$ 95:5, v/v); ^{1}H NMR (500 MHz, $CDCl_3$): $\delta=8.51$ (d, ^3J(H,H)=8.0 Hz, 2H; 2×H_2(Dans)), 8.30 (d, ^3J(H,H)=8.5 Hz, 2H; 2×H_8(Dans)), 8.22 (d, ^3J(H,H)=7.0 Hz, 2H; 2×H_4(Dans)), 7.55–7.02 (complex signals, 16H; 2×H_3(Dans), 2×H_6(Dans), 2×H_7(Dans) and phenyl protons), 5.64–5.59 (brs, exchangeable protons, 2H; 2×N*H*−*TEG*), 5.53 (s, 1H; Ph−C*H*), 5.06 (d, ^3J(H,H)=7.5 Hz, 1H; H-1), 4.33 (m, 1H; H-4), 4.07–3.91 (overlapped signals, 5H; -CH_2-O-C-2, -CH_2-O-C-3 and H-6_a), 3.76 (t, ^3J(H,H)=10.5 and 10.0 Hz, 1H; H-3), 3.66–3.49 (overlapped signals, 23H; 10×O-CH_2-*TEG*, H-6_b, H-2 and H-5), 3.36–3.31 (m, 4H; 2×CH_2-CH_2-$NHSO_2$-), 3.10–3.06 (m, 4H; 2×-CH_2-CH_2-$NHSO_2$-), 2.87 ppm (s, 12H; 4×CH_3-*N*-Dans); ^{13}C NMR (75 MHz, $CDCl_3$): $\delta=132.1$, 129.4, 128.9, 128.5, 128.1, 126.0, 122.8 and 116.9 (aromatic carbons), 101.4 (C-1), 101.1 (Ph−*C*H), 82.5 (C-2), 81.5 and 80.4 (2×-CH_2-CH_2-O-sugar), 72.5 and 72.3 (2×-CH_2-O-sugar), 70.6 and 70.4 (10×O-CH_2 *TEG*), 70.2 (C-6), 69.2 (C-3), 68.5 (C-4), 66.0 (C-5), 45.8 (4×CH_3-*N*-Dans), 43.0 ppm (2×CH_2-CH_2-$NHSO_2$); IR (KBr): $\tilde{\nu}_{max}=3494$ (broad), 1593, 1494, 1459, 1325, 1223, 1142, 1089, 768, 699 cm^{-1}; MS (ESI$^+$): *m/z*: calcd for $C_{59}H_{76}N_4O_{16}S_2$: 1160.47; found: 1161.65 $[M+H]^+$, 1183.64 $[M+Na]^+$, 1199.69 $[M+K]^+$; HRMS (MALDI-TOF): *m/z*: calcd for $C_{59}H_{76}N_4O_{16}S_2Na$: 1183.4595; found: 1183.4612 $[M+Na]^+$.

Synthesis of tryptophan-tagged derivative 10b: Compound **9** (130 mg, 0.19 mmol), previously dried by repeated coevaporations with anhydrous benzene and kept under reduced pressure, was dissolved in anhydrous CH_2Cl_2 (3 mL). DIPEA (163 μL, 0.76 mmol), DCC (235 mg, 1.14 mmol) and Fmoc-protected tryptophan (240 mg, 0.57 mmol) were sequentially added and the resulting solution was left stirring overnight at room temperature. The reaction mixture was then concentrated under reduced pressure, transferred into a separating funnel and washed twice with a saturated NaCl solution. The organic phase, dried over anhydrous Na_2SO_4, was filtered, concentrated under reduced pressure and then chromatographed on a silica gel column. Elution with $CHCl_3$ containing increasing amounts of CH_3OH (from 0% to 10%), allowed product **10b** to be isolated in a pure form (235 mg, 0.16 mmol) in 84% yield. Oil, $R_f=0.5$ ($CHCl_3/CH_3OH$ 9:1, v/v); ^1H NMR (500 MHz, $CDCl_3$): $\delta=7.76$–6.95 (complex signals, 38H; aromatic protons), 6.00 (brs, exchangeable protons, 2H; 2×N*H*–*TEG*), 5.84 (brs, exchangeable protons, 2H; 2×N*H*-*Trp*), 5.29 (s, 1H; Ph–C*H*), 4.88 (d, ^3J(H,H)=7.0 Hz, 1H; H-1), 4.45–4.33 (overlapped signals, 6H; 2×CH_2-Fmoc and 2×CH-*Trp*), 4.26 (m, 1H; H-4), 4.21 (m, 2H; 2×CH-Fmoc), 4.02–3.79 (overlapped signals, 5H; -CH_2-O-C-2, -CH_2-O-C-3 and H-6_a), 3.66–3.18 (overlapped signals, 31H; H-3, 12×O-CH_2 *TEG*, 2×CH_2-*Trp*, H-2 and H-6_b), 3.11–3.05 ppm (overlapped signals, 5H; 2×-CH_2-NHCO and H-5); ^{13}C NMR (125 MHz, $CDCl_3$): $\delta=$ 171.0 (CO), 156.8, 155.7, 143.7, 141.1, 137.1, 136.2, 129.4, 128.9, 128.1, 127.6, 127.3, 127.0, 126.0, 125.0, 123.7, 122.8, 121.8, 119.8, 119.4, 118.7, 116.6, 111.4 and 109.9 (aromatic carbons), 101.2 (C-1), 101.0 (Ph–*C*H), 82.3 (C-2), 81.4 and 80.3 (2×-*C*H_2-CH_2-O-sugar), 72.1 and 71.9 (2×-*C*H_2-O-sugar), 70.6, 70.4, 70.2 and 70.1 (10×O-*C*H_2 *TEG*), 69.9 (C-3), 69.2 (C-6), 68.4 (C-4), 66.8 (CH_2-Fmoc), 65.8 (C-5), 55.5 (*C*H-α *Trp*), 47.0 (*C*H-Fmoc), 39.1 (2×-*C*H_2-NHCO), 29.6 ppm (*C*H_2-*Trp*); IR (KBr): $\tilde{\nu}_{max}=$ 3412 and 3297 (broad), 1703, 1663, 1499, 1455, 1228, 1085, 743 cm^{-1}; MS (ESI^+): *m/z*: calcd for $C_{87}H_{94}N_6O_{18}$: 1510.6625; found: 1535.96 $[M+Na]^+$, 1552.05 $[M+K]^+$; HRMS (MALDI-TOF): *m/z*: calcd for $C_{87}H_{94}N_6O_{18}Na$: 1533.6522; found: 1533.6539 $[M+Na]^+$.

Synthesis of ferrocene-tagged derivative 10c: Compound **9** (130 mg, 0.19 mmol), previously dried by repeated coevaporations with anhydrous benzene and kept under reduced pressure, was dissolved in anhydrous CH_2Cl_2 (3 mL). DIPEA (130 μL, 0.76 mmol), DCC (235 mg, 1.1 mmol), and ferrocenecarboxylic acid (132 mg, 0.57 mmol) were sequentially added and the resulting solution was left stirring overnight at room temperature. The reaction mixture was then concentrated under reduced pressure, transferred into a separating funnel and washed twice with a saturated NaCl solution. The organic phase, dried over anhydrous Na_2SO_4, was filtered, concentrated under reduced pressure and then chromatographed on a silica gel column. Elution with $CHCl_3$ containing increasing amounts of CH_3OH (from 0% to 10%) gave product **10c** (150 mg, 0.13 mmol) in 68% yield. Oil, $R_f=0.3$ ($CHCl_3/CH_3OH$ 9:1, v/v); ^1H NMR (500 MHz, $CDCl_3$): $\delta=7.51$–7.03 (complex signals, 10H; aromatic protons), 6.12 (brs, exchangeable protons, 2×NH), 5.64 (s, 1H; Ph–C*H*), 5.30 (d, ^3J(H,H)=7.5 Hz, 1H; H-1), 4.94 (brs, 4H; H-3 and H-4 ferrocene rings A), 4.34 (m, 1H; H-4), 4.28 (brs, 4H; H-2 and H-5 ferrocene rings A), 4.19 (s, 10H; ferrocene unsubstituted rings B), 4.05–3.95 (overlapped signals, 5H; -CH_2-O-C-2, -CH_2-O-C-3 and H-6_a), 3.84–3.49 (overlapped signals, 26H; H-3, 12×O-CH_2 TEG and H-6_b), 3.42–3.38 (m, 2H; H-2 and H-5), 3.08–3.03 ppm (m, 4H; 2×-CH_2-NHCO); ^{13}C NMR (100 MHz, $CDCl_3$): $\delta=170.8$ (CO), 156.8, 137.2, 130.3, 129.7, 128.9, 128.7, 128.1, 127.3, 127.0, 125.4, 123.7, 122.0, 117.5 and 115.9 (aromatic carbons), 102.1 (Ph–*C*H), 100.4 (C-1), 83.3 (C-2), 81.8 and 80.4 (2×*C*H_2-CH_2-O-sugar), 79.4 (ferrocene ring B carbons), 71.5 and 71.1 (2×-*C*H_2-O-sugar), 70.5, 70.1, 69.3 and 68.8 (10×O-*C*H_2 *TEG* and ferrocene ring A carbons), 67.7 (C-3), 66.7 (C-4), 66.2 (C-5), 65.2 (C-6), 40.7 ppm (2×*C*H_2–NHCO); IR (KBr): $\tilde{\nu}_{max}=$3410 and 3290 (broad), 1635, 1540, 1490, 1452, 1226, 1085, 1024, 733, 696 cm^{-1}; MS (ESI^+): *m/z*: calcd for $C_{57}H_{70}N_2Fe_2O_{14}$: 1118.3526; found: 1141.34 $[M+Na]^+$, 1157.36 $[M+K]^+$; HRMS (MALDI-TOF): *m/z*: calcd for $C_{57}H_{70}N_2Fe_2O_{14}Na$: 1141.3424; found: 1141.3446 $[M+Na]^+$.

Synthesis of *N*-propargylamide of cholic acid (11): Cholic acid (1.0 g, 2.4 mmol) was dissolved in anhydrous CH_2Cl_2 (6 mL). DIPEA (640 μL, 3.7 mmol), DCC (760 mg, 3.7 mmol), HOBt (360 mg, 2.7 mmol) and propargylamine (185 μL, 2.7 mmol) were sequentially added to the stirred mixture, which was left at room temperature for 4 h. The reaction mixture was then diluted with $CHCl_3$, transferred into a separating funnel and washed twice with water. The organic phase, dried over anhydrous Na_2SO_4 and filtered, was then concentrated under reduced pressure and purified by column chromatography. Elution of the column with $CHCl_3$ containing increasing amounts of CH_3OH (from 1 to 10%) gave pure **11** (1.0 g, 2.2 mmol) in 92% yield. White amorphous solid, $R_f=0.6$ (CH_2Cl_2/CH_3OH 85:15, v/v); ^1H NMR (400 MHz, $CDCl_3$): $\delta=5.70$ (brs, 1H; exchangeable proton, NH), 4.05 (brs, 2H; CH_2–NH), 3.98, 3.86 and 3.47 (3×brs, each 1H; 3×C*H*OH), 2.23 (1H; H-alkyne), 2.27–1.15 (overlapped signals, 24H; CH_2 and C*H* protons of the cholic acid residue), 1.00, 0.92 and 0.71 ppm (3×s, each 3H; CH_3 protons of the cholic acid residue); ^{13}C NMR (50 MHz, $CDCl_3$): $\delta=174.0$ (CO), 79.9 (C_{sp}), 71.7 (CH_{sp}), 73.0, 71.0 and 68.3 (*C*HOH), 46.2 (*C*H_2–NH), 41.4, 39.2, 35.2, 34.6, 32.6, 31.4, 30.2, 28.9, 28.0, 27.5, 26.1 and 23.1 (*C*H_2 and *C*H carbons of the cholic acid residue), 22.3, 17.3 and 12.3 ppm (CH_3 carbons of the cholic acid residue); IR (KBr): $\tilde{\nu}_{max}=$3306 (broad), 1649, 1540, 1445, 1370, 1073, 1037, 754, 661 cm^{-1}; MS (ESI^+): *m/z*: calcd for $C_{27}H_{43}NO_4$: 445.3192; found: 468.71 $[M+Na]^+$, 484.59 $[M+K]^+$.

Cu^I-promoted 1,3-dipolar cycloaddition—synthesis of triazole 12: Compound **8** (84 mg, 0.11 mmol) and compound **11** (150 mg, 0.33 mmol) were dissolved in anhydrous DMF (1.0 mL). DBU (165 μL, 1.1 mmol) and CuI (63 mg, 0.33 mmol) were added to the stirred mixture, which was left at room temperature for 48 h. The reaction mixture was concentrated under reduced pressure, diluted with $CHCl_3$ and then transferred into a separating funnel and washed twice with water. The organic phase, dried over anhydrous Na_2SO_4 and filtered, was then concentrated under reduced pressure and the resulting residue was purified by column chromatography. Elution of the column with $CHCl_3$ containing increasing amounts of CH_3OH (from 1 to 10%) gave pure **12** (165 mg, 0.10 mmol) in 92% yield. Oil, $R_f=0.6$ (CH_2Cl_2/CH_3OH 85:15, v/v); ^1H NMR (500 MHz, $CDCl_3$): $\delta=7.44$–7.01 (complex signals, 12H; aromatic protons), 5.57 (s, 1H; Ph–C*H*), 5.02 (d, ^3J(H,H)=7.6 Hz, 1H; H-1), 4.56 (brs, exchangeable protons, 2×NH), 4.37 (m, 1H; H-4), 4.32–3.70 (overlapped signals, 8H; -CH_2-O-C-2, -CH_2-O-C-3 and 2×CH_2–NHCO), 3.63–3.40 (overlapped signals, 35H; 12×O-CH_2 *TEG*, 6×C*H*OH of the cholic acid residues, H-3, H_2-6, H-2 and H-5), 2.90 (brs, 4H; 2×-CH_2-N *TEG*), 2.40–1.20 (overlapped signals, 48H; CH_2 and C*H* protons of the cholic acid residues), 0.85, 0.66 and 0.63 ppm (3×s, each 6H; CH_3 protons of the cholic acid residues); ^{13}C NMR (50 MHz, $CDCl_3$): $\delta=166.3$ (CO), 157.2, 145.8, 137.3, 129.4, 128.8, 128.0, 126.0, 122.9, 117.1 (aromatic carbons), 101.9 (C-1), 101.2 (Ph–*C*H), 82.5 (C-2), 81.7 and 80.7 (2×-*C*H_2-CH_2-O-sugar), 72.4 and 72.3 (2×-*C*H_2-O-sugar), 72.9, 71.8 and 68.2 (*C*HOH of the cholic acid residues), 70.5 (10×O–*C*H_2 *TEG*), 68.8 (C-3), 68.6 (C-4), 66.2 (C-5), 62.8 (C-6), 54.4 (N–*C*H_2 *TEG*), 46.5 (*C*H_2–NHCO), 48.7, 41.6, 39.7, 37.9, 35.3, 34.7, 32.2, 31.4, 30.5, 28.9, 27.5, 26.7, 23.9, 23.2 and 22.4 (*C*H_2 and *C*H carbons of the cholic acid residues), 19.5, 17.4 and 12.4 ppm (CH_3 carbons of the cholic acid residues); IR (KBr): $\tilde{\nu}_{max}=$3365 (broad), 1646, 1540, 1455, 1375, 1222, 1077, 1043, 756, 661 cm^{-1}; MS ($MALDI^+$): *m/z*: calcd for $C_{89}H_{136}N_8O_{20}$: 1636.9871; found: 1637.48 $[M+H]^+$, 1676.63 $[M+K]^+$; HRMS (MALDI-TOF): *m/z*: calcd for $C_{89}H_{136}N_8O_{20}Na$: 1659.9769; found: 1659.9806 $[M+Na]^+$.

Removal of benzylidene group—synthesis of 14: Compound **10a** (170 mg, 0.15 mmol), dissolved in anhydrous THF (1.3 mL), was treated with sodium hydride (18 mg, 0.44 mmol) and the reaction mixture was left stirring for 10 min. Methyl iodide (20 μL, 0.33 mmol) was then added and the resulting system was left overnight at room temperature. The reaction mixture was then concentrated under reduced pressure, diluted with $CHCl_3$, transferred into a separating funnel and washed twice with water. The organic phase was then taken to dryness, which gave target compound **13** in a pure form and almost quantitative yields. Derivative **13** (170 mg, 0.15 mmol) was then treated with a TFA/CH_2Cl_2/H_2O (1:10:0.5 v/v/v) solution (10 mL) and the resulting mixture was left at 0°C. After 4 h, the reaction mixture was diluted with $CHCl_3$. The organic phase was washed twice with water and concentrated under reduced pressure. The crude product was purified by column chromatography. Elution of the column with $CHCl_3$ containing increasing amounts of CH_3OH (from 1 to 5%) gave pure **14** (160 mg, 0.15 mmol) in almost quantitative yields. Oil, $R_f=0.3$ ($CHCl_3/CH_3OH$ 95:5, v/v); ^1H NMR

(500 MHz, $CDCl_3$): $\delta = 8.52$ (d, $^3J(H,H) = 8.5$ Hz, 2H; 2×H_2(Dans)), 8.33 (d, $^3J(H,H) = 8.5$ Hz, 2H; 2×H_8(Dans)), 8.14 (m, 2H; 2×H_4(Dans)), 7.53 (m, 4H; 2×H_3(Dans) and 2×H_7(Dans)), 7.17 (d, $^3J(H,H) = 7.5$ Hz, 2H; 2×H_6(Dans)), 7.27–6.98 (complex signals, 5H; phenyl protons), 4.95 (d, $^3J(H,H) = 7.0$ Hz, 1H; H-1), 4.12 (m, 1H; H-4), 4.07–3.72 (overlapped signals, 6H; -CH_2-O-C-2, -CH_2-O-C-3 and H_2-6), 3.66–3.52 (overlapped signals, 25H; 12×O−CH_2 *TEG* and H-3), 3.44 (m, 4H; N−CH_2 *TEG*), 3.41 (t, $J = 5.5$ and 5.5 Hz, 1H; H-5), 3.38 (m, 1H; H-2), 2.94 and 2.93 (2×s, each 3H; 2×-CH_2-NCH_3SO_2-), 2.87 ppm (s, 12H; 4×CH_3-*N*-Dans); ^{13}C NMR (50 MHz, $CDCl_3$): $\delta = 157.1$, 151.7, 134.7, 130.1, 129.4, 127.8, 123.0, 119.7, 116.7 and 115.2 (aromatic carbons), 101.4 (C-1), 85.9 (C-2), 82.0 (C-5), 75.6 (C-3), 72.2 and 71.9 (2×CH_2-O-sugar), 71.9, 70.5, 70.4 and 70.2 (12×O−CH_2 *TEG*), 62.8 (C-6), 60.1 (C-4), 49.2 (2×N−CH_2 *TEG*), 45.2 (4×CH_3-*N*-Dans), 35.7 ppm (2×-CH_2-NCH_3SO_2-); IR (KBr): $\tilde{\nu}_{max} = 3451$ (broad), 1589, 1574, 1452, 1324, 1229, 1142, 1070, 983, 933, 774, 695 cm^{-1}. MS (MALDI$^+$): *m/z*: calcd for $C_{54}H_{76}N_4O_{16}S_2$: 1100.4698; found: 1101.14 $[M+H]^+$, 1123.27 $[M+Na]^+$, 1139.24 $[M+K]^+$; HRMS (MALDI-TOF): *m/z*: calcd for $C_{54}H_{76}N_4O_{16}S_2Na$: 1123.4595; found: 1123.4630 $[M+Na]^+$.

Synthesis of 15: Compound **14** (160 mg, 0.15 mmol), dissolved in anhydrous pyridine (2.0 mL), was treated with DMTCl (60 mg, 0.18 mmol). The reaction mixture, left at room temperature overnight with stirring, was then diluted with CH_3OH and concentrated under reduced pressure. The crude product was next purified on a silica gel column. Elution with CH_2Cl_2 containing increasing amounts of CH_3OH (from 1 to 5%) in the presence of a few drops of pyridine gave pure **15** (210 mg, 0.15 mmol) in almost quantitative yield. Glassy solid, m.p. dec. > 90°C. $R_f = 0.8$ ($CHCl_3$/CH_3OH 95:5, v/v). ^{1}H NMR (500 MHz, $CDCl_3$): $\delta = 8.52$ (d, $^3J(H,H) = 8.5$ Hz, 2H; 2×H_2(Dans)), 8.33 (d, $^3J(H,H) = 8.5$ Hz, 2H; 2×H_8(Dans)), 8.14 (m, 2H; 2×H_4(Dans)), 7.52 (m, 4H; 2×H_3(Dans) and 2×H_7(Dans)), 7.49–6.71 (complex signals, 20H; DMT aromatic protons, phenyl protons and 2×H_6(Dans)), 4.95 (d, $^3J(H,H) = 8.0$ Hz, 1H; H-1), 4.13–3.71 (overlapped signals, 5H; -CH_2-O-C-2, -CH_2-O-C-3 and H-4), 3.74 (s, 6H; OCH_3 of the DMT group), 3.65–3.53 (overlapped signals, 26H; 12×O−CH_2 *TEG* and H_2-6), 3.47–3.42 (overlapped signals, 6H; 2×N−CH_2 *TEG*, H-3 and H-5), 3.38 (t, 1H; H-2), 2.94 and 2.91 (2×s, each 3H; 2×-CH_2-NCH_3SO_2-), 2.87 ppm (s, 12H; 4×CH_3-*N*-Dans); ^{13}C NMR ($CDCl_3$, 50 MHz): $\delta = 158.2$, 157.2, 151.6, 144.9, 139.4, 136.1, 134.4, 130.0, 129.3, 129.0, 128.2, 127.7, 126.9, 126.4, 123.0, 122.4, 119.6, 116.9, 115.1, 113.1 and 112.9 (aromatic carbons), 101.2 (C-1), 86.3 (quaternary C of DMT group), 85.8 (C-2), 82.1 (C-5), 75.3 (C-3), 72.3 and 71.9 (2×CH_2-O-sugar), 70.5, 70.4 and 69.9 (12×O×CH_2 *TEG* and, overlapped, C-4), 63.4 (C-6), 55.1 (OCH_3 of the DMT group), 49.1 (2×N−CH_2 *TEG*), 46.2 and 45.3 (4×CH_3-*N*-Dans), 35.8 ppm (2×-CH_2-NCH_3SO_2-); IR (KBr): $\tilde{\nu}_{max} =$ 1608, 1511, 1453, 1301, 1247, 1142, 1080, 1030, 820, 787, 700 cm^{-1}; MS (ESI$^+$): *m/z*: calcd for $C_{75}H_{94}N_4O_{18}S_2$: 1402.6004; found: 1425.66 $[M+Na]^+$, 1441.68 $[M+K]^+$; HRMS (MALDI-TOF): *m/z*: calcd for $C_{75}H_{94}N_4O_{18}S_2Na$: 1425.5902; found: 1425.5980 $[M+Na]^+$.

Synthesis of 16: Compound **15** (200 mg, 0.14 mmol), dissolved in anhydrous CH_2Cl_2 (2 mL) and previously left in contact with activated molecular sieves (3 Å), was treated with DIPEA (145 mL, 0.84 mmol) and 2-cyanoethyl-*N*,*N*-diisopropylchlorophosphoramidite (100 mL, 0.45 mmol), sequentially added with stirring at room temperature. After 2 h, the reaction mixture was concentrated under reduced pressure. The crude product was then chromatographed on a silica gel column, with elution with *n*-hexane containing increasing amounts of ethyl acetate (from 30 to 50%) in the presence of a few drops of triethylamine, furnishing the desired compound **16** (200 mg, 0.13 mmol) in 90% yield. Oil, as a mixture of diastereomers: $R_f = 0.5$ (CH_2Cl_2/CH_3OH, 99:1, v/v); ^{1}H NMR (300 MHz, $CDCl_3$): $\delta = 8.52$ (d, $^3J(H,H) = 8.5$ Hz, 4H; 4×H_2(Dans)), 8.33 (d, $^3J(H,H) = 8.5$ Hz, 4H; 4×H_8(Dans)), 8.13 (d, $^3J(H,H) = 7.5$ Hz, 4H; 4×H_4(Dans)), 7.51 (m, 8H; 4×H_3(Dans) and 4×H_7(Dans)), 7.44–6.69 (complex signals, 40H; DMT aromatic protons, phenyl protons and 4×H_6(Dans)), 4.97 (m, 2H; 2×H-1), 4.32–3.85 (overlapped signals, 16H; 2×-O-CH_2-CH_2-CN, 4×-CH_2-O-sugar, 2×H-6_a, 2×H-4), 3.79 (s, 12H; 4×OCH_3 of *DMT* group), 3.76–3.37 {overlapped signals, 68H; 2×H-6_b, 2×H-3, O-CH_2-CH_2-O *TEG*, 2×H-2, 2×H-5 and 4×N[$CH(CH_3)_2$]$_2$}, 2.93 (s, 12H; 4×-CH_2-NCH_3SO_2-), 2.86 (s, 24H; 8×CH_3-*N*-Dans), 2.73 (t, 4H; 2×-O-CH_2-CH_2-CN), 1.28, 1.27, 1.26, 1.25, 1.22, 1.20, 0.98 and 0.96 ppm {2×s, each 3H; 24H; 2×N[$CH(CH_3)_2$]$_2$}. ^{13}C NMR (75 MHz, $CDCl_3$): $\delta =$ 158.2, 151.6, 145.0, 139.4, 134.4, 130.1, 129.3, 129.0, 128.2, 127.8, 127.7, 126.5, 123.0, 119.6, 116.8, 115.1, 113.1, 112.9 and 112.1 (aromatic carbons), 116.8 (CN), 101.0 (C-1), 85.8 (quaternary C of *DMT* group), 84.0 and 82.4 (C-2 and C-5), 75.3 (C-3), 72.3 and 71.9 (2×CH_2-O-sugar), 70.4, 70.3 and 69.8 (O-CH_2-CH_2-O *TEG* and, overlapped, C-4), 63.7 and 63.5 (C-6), 58.0 (-O-CH_2-CH_2-CN), 55.0 (OCH_3 of *DMT* group), 49.1 (2×N−CH_2 *TEG*), 46.7 (4×CH_3-*N*-Dans), 42.9 {N[$CH(CH_3)_2$]$_2$}, 35.7 (2×-CH_2-NCH_3SO_2-), 24.3 and 22.2 {N[$CH(CH_3)_2$]$_2$}, 19.9 and 19.1 ppm (-O-CH_2-CH_2-CN); ^{31}P NMR (161.98 MHz, $CDCl_3$): $\delta = 151.0$ and 150.4 ppm; IR (KBr): $\tilde{\nu}_{max} = 2252$, 1606, 1507, 1457, 1324, 1217, 1138, 1027, 973, 765 cm^{-1}; MS (ESI$^+$): *m/z*: calcd for $C_{84}H_{111}N_6O_{19}PS_2$: 1602.7083; found: 1605.02 $[M+H]^+$, 1705.12 $[M+Et_3NH]^+$; HRMS (MALDI-TOF): *m/z*: calcd for $C_{84}H_{111}N_6O_{19}PS_2Na$: 1625.6981; found: 1625.6997 $[M+Na]^+$.

Synthesis of 4-*O*-(2-chlorophenylphosphate) derivative 17: 2-Chlorophenyl-dichlorophosphate (228 mL, 1.40 mmol, 4 equiv) was added dropwise at 0°C to a stirred solution of compound **15** (500 mg, 0.35 mmol, 1 equiv), 1,2,4-triazole (193 mg, 2.80 mmol, 8 equiv) and triethylamine (390 μL, 2.80 mmol, 8 equiv) in anhydrous pyridine (9.0 mL). The mixture was allowed to warm to room temperature. After 3 h the reaction mixture was concentrated under reduced pressure. The crude product was then diluted with $CHCl_3$, transferred into a separating funnel, washed three times with water, concentrated under reduced pressure and purified by column chromatography. Elution with CH_2Cl_2 containing increasing amounts of CH_3OH (from 1 to 10%), with the addition of a few drops of TFA, afforded pure **17** (395 mg, 0.30 mmol) in 86% yield. Oil. $R_f = 0.3$ ($CHCl_3$/CH_3OH, 98:2, v/v). ^{1}H NMR (500 MHz, $CDCl_3$): $\delta = 8.51$ (d, $^3J(H,H) = 9.0$ Hz, 2H; 2×H_2(Dans)), 8.31 (d, $^3J(H,H) = 9.0$ Hz, 2H; 2×H_8(Dans)), 8.12 (d, $^3J(H,H) = 7.5$ Hz, 2H; 2×H_4(Dans)), 7.49 (m, 4H; 2×H_3(Dans) and 2×H_7(Dans)), 7.30–6.90 (complex signals, 11H; phenyl protons and 2×H_6(Dans)), 4.78 (d, $^3J(H,H) = 7.0$ Hz, 1H; H-1), 4.48 (m, 1H; H-4), 4.00 (m, 2H; CH_2-O-sugar), 3.91 (d, $^3J(H,H) = 12.0$ Hz, 1H; H-6_a), 3.75–3.68 (overlapped signals, 3H; CH_2-O-sugar and H-6_b), 3.64–3.38 (overlapped signals, 30H; H-3, H-2 and O-CH_2-CH_2-O *TEG*), 3.30 (m, 1H; H-5), 2.90 (s, 6H; 2×-CH_2-NCH_3SO_2-), 2.86 and 2.81 ppm (s, 12H; 4×CH_3-*N*-Dans); ^{13}C NMR (125 MHz, $CDCl_3$): $\delta = 157.3$, 151.6, 149.5, 134.3, 130.5, 130.1, 130.0, 129.8, 129.7, 129.4, 129.2, 128.6, 127.9, 127.1, 125.4, 123.4, 123.0, 122.3, 122.1, 119.5, 118.9, 116.8 and 115.0 (aromatic carbons), 101.5 (C-1), 85.1 (C-2), 82.0 (C-3), 76.0 (C-5), 72.6 (C-4), 71.5 and 70.9 (2×CH_2-O-sugar), 70.3, 70.2, 70.1, 69.7 and 69.2 (O-CH_2-CH_2-O *TEG*), 61.0 (C-6), 49.2 and 49.0 (2×N−CH_2 *TEG*), 46.1 and 45.3 (4×CH_3-*N*-Dans), 35.7 ppm (2×-CH_2-NCH_3SO_2-)]; ^{31}P NMR (161.98 MHz, $CDCl_3$): $\delta = -6.8$ ppm; HRMS (MALDI-TOF): *m/z*: calcd for $C_{60}H_{80}ClN_4O_{19}PS_2$: 1290.4284; found: 1289.3460 $[M-H]^-$.

Synthesis of DMT-free linear dimer 18: Derivative **17** (150 mg, 0.12 mmol, 1 equiv) and compound **16** (228 mg, 0.14 mmol, 1.2 equiv), previously dried by repeated coevaporations with anhydrous CH_3CN and kept under reduced pressure, were treated with a DCI solution (0.25 M) in anhydrous CH_3CN (5.0 mL). The reaction was left stirring and monitored by TLC in the eluent system $CHCl_3$/CH_3OH 96:4 v/v. After 2.0 h, a *t*BuOOH solution in *n*-decane (5.5 M, 0.3 mL) was added to the mixture, which was left stirring at room temperature. After an additional 30 min the reaction mixture was diluted with $CHCl_3$, transferred into a separating funnel and washed three times with water. The organic phase, concentrated under reduced pressure, was then purified by column chromatography. Elution with CH_2Cl_2 containing increasing amounts of CH_3OH (from 1 to 10%) in the presence of a few drops of TFA afforded pure **18** (218 mg, 0.087 mmol) in 72% yield. Oil. $R_f = 0.5$ ($CHCl_3$/CH_3OH 98:2, v/v). ^{1}H NMR (400 MHz, $CDCl_3$): $\delta = 8.52$ (d, $^3J(H,H) = 8.5$ Hz, 4H; 4×H_2(Dans)), 8.33 (d, $^3J(H,H) = 8.5$ Hz, 4H; 4×H_8(Dans)), 8.13 (m, 4H; 4×H_4(Dans)), 7.50 (m, 8H; 4×H_3(Dans) and 4×H_7(Dans)), 7.24–6.90 [complex signals, 18H; phenyl protons and 4×H_6(Dans)], 4.89 and 4.80 (2×m, each 1H; H-1 and H-1′), 4.23 (t, 2H; O-CH_2-CH_2-CN), 4.10–3.09 (overlapped signals, 74H; H_2-6-O-P, 2×H-4, 2×H-3 and 2×H-5, 32×O−CH_2 *TEG* and H_2-6-OH), 3.40 and 3.38 (obscured, 2H; 2×H-2), 2.91 (s, 12H; 4×-CH_2-NCH_3SO_2-), 2.85 (s, 24H; 8×CH_3-*N*-Dans), 2.49–2.37 ppm (m, 2H; O-CH_2-CH_2-CN; ^{13}C NMR (100 MHz, $CDCl_3$): $\delta = 165.1$, 156.9, 151.6, 144.9, 134.4, 134.2, 130.8, 130.2, 130.0, 129.4, 128.7, 127.9, 123.0, 122.6, 121.6, 119.5, 116.6, 116.4, 115.1 (aromatic carbons), 116.1 (CN),

100.6 and 100.2 (2×C-1), 84.2 and 84.0 (2×C-2), 81.7 and 81.6 (2×C-5), 75.3 (2×C-3), 74.0 and 73.8 (4×*C*H_2-O-sugar), 71.7, 70.2, 69.5 and 69.2 (28×O−*C*H_2 *TEG* and, overlapped, 2×C-4), 68.0 (C-6-O-P), 62.5 (C-6-OH), 60.3 (-O-*C*H_2-CH_2-CN), 49.1 (4×N−*C*H_2 *TEG*), 45.5 and 45.3 (8×*C*H_3-*N*-Dans), 35.6 (4×-CH_2-N*C*$H_3$$SO_2$-), 29.6 ppm (-O-$CH_2$-*C*$H_2$-CN); ^{31}P NMR (161.98 MHz, $CDCl_3$): broad signals centred at $\delta = -3.1$ and -7.4 ppm; HRMS (MALDI$^-$-TOF): *m*/*z*: calcd for $C_{117}H_{158}ClN_9O_{37}P_2S_4$: 2505.8805; found: 2503.2009 $[M-H]^-$.

Synthesis of fully protected cyclic dimer 19: Derivative **18** (30 mg, 0.012 mmol, 1 equiv), previously dried by repeated coevaporations with anhydrous pyridine, DMAP (3.0 mg, 0.024 mmol, 2 equiv) and MSNT (106 mg, 0.36 mmol, 30 equiv) were dissolved in anhydrous pyridine (12 mL) and left two days with stirring at room temperature. The reaction mixture was then concentrated under reduced pressure, dissolved in ethyl acetate, transferred into a separating funnel and washed three times with water. The organic phase was concentrated under reduced pressure and purified by column chromatography with elution with $CHCl_3$ containing increasing amounts of CH_3OH (from 1 to 15%), affording pure **19** (22 mg, 0.009 mmol) in 75% yield. Oil, $R_f = 0.5$ ($CHCl_3$/CH_3OH 95:5, v/v). ^{1}H NMR (400 MHz, $CDCl_3$): $\delta = 8.59$ (d, ^3J(H,H) = 8.0 Hz, 4H; 4×H_2(Dans)), 8.37 (d, ^3J(H,H) = 8.0 Hz, 4H; 4×H_8(Dans)), 8.13 (m, 4H; 4×H_4(Dans)), 7.53 (m, 8H; 4×H_3(Dans) and 4×H_7(Dans)), 7.28–6.84 (complex signals, 18H; phenyl protons and 4×H_6(Dans)), 5.06 and 4.86 (2×m, each 1H: H-1 and H-1′), 4.34 (overlapped signals, 8H; 4×CH_2-C*H_2*-O-sugar), 4.07 (t, 2H; O-C*H_2*-CH_2-CN), 3.97–3.39 (overlapped signals, 72H; H_2-6-O-P, 2×H-4, 2×H-3, 2×H-5, 28×O−C*H_2 TEG* and H_2-6-OH), 3.37 and 3.28 (obscured, 2H; 2×H-2), 2.99 (s, 12H; 4×-CH_2-NC*H_3*SO_2-), 2.92 (s, 24H; 8×C*H_3*-*N*-Dans), 2.40–2.34 ppm (m, 2H; O-CH_2-C*H_2*-CN); ^{13}C NMR (125 MHz, $CDCl_3$): $\delta = 165.0$, 158.1, 157.0, 156.9, 151.5, 149.4, 144.6, 135.7, 135.6, 134.2, 130.1, 130.0, 129.9, 129.4, 129.2, 129.0, 127.9, 127.7, 127.6, 127.4, 126.5, 123.1, 122.9, 122.5, 121.5, 119.5, 119.4, 116.7 and 115.0 (aromatic carbons), 116.1 and 116.0 (CN), 100.6 and 100.3 (2×C-1), 85.9 and 85.7 (2×C-2), 81.9 and 81.2 (2×C-5), 73.8 (2×C-3), 72.0 and 71.9 (4×*C*H_2-O-sugar), 70.2 and 69.7 (28×O-*C*H_2 *TEG* and, overlapped, 2×C-4), 62.6 (C-6), 60.3 (-O-*C*H_2-CH_2-CN), 48.9 (2×N−*C*H_2 *TEG*), 45.8, 45.7, 45.6, 45.4, 45.3 and 45.2 (4×*C*H_3-*N*-Dans), 35.7 and 35.6 (2×-CH_2-N*C*$H_3$$SO_2$-), 22.9 ppm (-O-$CH_2$-*C*$H_2$-CN); ^{31}P NMR (161.98 MHz, $CDCl_3$): $\delta = -2.1$, -5.0, -9.5 and -10.6 ppm; HRMS (MALDI$^+$-TOF): *m*/*z*: calcd for $C_{117}H_{156}ClN_9O_{36}P_2S_4$: 2487.8700; found: 2487.1564 $[M+H]^+$, 2509.0653 $[M+Na]^+$.

Synthesis of partially protected cyclic dimer 20: Compound **19** (22 mg, 0.009 mmol) was treated with piperidine (1.0 mL) and the resulting mixture was left overnight with stirring at 70 °C. The reaction was quenched by removal of the solvent in vacuo. The crude product was then purified by column chromatography with elution with $CHCl_3$ containing increasing amounts of CH_3OH (from 1 to 15%), affording pure **20** (21 mg, 0.0086 mmol) in 96% yields. Oil, $R_f = 0.3$ ($CHCl_3$/CH_3OH 95:5 v/v); ^{1}H NMR (400 MHz, $CDCl_3$): $\delta = 8.52$ (d, ^3J(H,H) = 8.0 Hz, 4H; 4×H_2-(Dans)), 8.33 (d, ^3J(H,H) = 8.0 Hz, 4H; 4×H_8(Dans)), 8.11 (m, 4H; 4×H_4(Dans)), 7.49 (m, 8H; 4×H_3(Dans) and 4×H_7(Dans)), 7.30–6.87 (complex signals, 18H; phenyl protons and 4×H_6(Dans)), 5.16 and 4.90 (2×m, each 1H; H-1 and H-1′), 4.40–3.35 (overlapped signals, 76H; 2×H_2-6, 2×H-4, O-CH_2-CH_2-O *TEG*, 2×H-2, 2×H-3 and 2×H-5), 2.98 (s, 12H; 4×CH_2-NC*H_3*SO_2-), 2.86 ppm (s, 24H; 8×C*H_3*-*N*-Dans); ^{13}C NMR (100 MHz, $CDCl_3$): $\delta = 165.1$, 158.0, 153.9, 142.4, 139.1, 134.9, 130.5, 129.4, 128.2, 124.8, 123.1, 122.6, 119.6, 117.2 and 115.1 (aromatic carbons), 101.4 and 101.1 (C-1 and C-1′), 84.7 (C-5 and C-5′), 75.9 (C-4 and C-4′), 71.9, 70.3 and 69.8 (O-*C*H_2-*C*H_2-O *TEG*), 61.6 (C-6), 49.0 (2×N−*C*H_2 *TEG*), 45.3 and 45.2 (4×*C*H_3-*N*-Dans), 35.8 and 35.6 ppm (2×CH_2-N*C*$H_3$$SO_2$-); ^{31}P NMR (161.98 MHz, $CDCl_3$): two broad signals, centred at $\delta = 0.7$ and -8.6 ppm; HRMS (MALDI$^-$-TOF): *m*/*z*: calcd for $C_{114}H_{153}ClN_8O_{36}P_2S_4$: 2434.8434; found: 2434.3841 $[M-H]^-$.

Synthesis of fully deprotected cyclic dimer 21: Compound **20** (21 mg, 0.0086 mmol), dissolved in dioxane (200 μL), was treated with saturated aq. LiOH solution (1.0 mL) and the resulting mixture was left overnight with stirring at 70 °C. The reaction mixture was then concentrated under reduced pressure, redissolved in $CHCl_3$, transferred into a separating funnel and washed three times with water. The organic phase was concentrated under reduced pressure and purified by column chromatography. Elution of the column with CH_2Cl_2 containing increasing amounts of CH_3OH (from 0 to 15%) gave pure cyclic dimer **21** (20 mg, 0.0086 mmol) in an almost quantitative yield. Oil, $R_f = 0.5$ ($CHCl_3$/CH_3OH 9:1 v/v); ^{1}H NMR (500 MHz, $CDCl_3$): $\delta = 8.78$ (broad, 4H; 4×H_2(Dans)), 8.19 (broad, 4H; 4×H_8(Dans)), 8.04 (broad, 4H; 4×H_4-(Dans)), 7.69 (broad, 8H; 4×H_3(Dans) and 4×H_7(Dans)), 7.52 (broad, 4H; 4×H_6(Dans)), 7.34–6.90 (complex signals, 10H; phenyl protons), 5.36–4.92 (m, 2H; H-1 and H-1′), 4.40–3.37 (overlapped signals, 74H; 2×H_2-6, 2×H-4, O-CH_2-CH_2-O *TEG*, 2×H-2 and 2×H-3), 3.11 (m, 2H; 2×H-5), 2.97 (s, 12H; 4×-CH_2-NC*H_3*SO_2-), 2.93 ppm (s, 24H; 8×C*H_3*-*N*-Dans); ^{13}C NMR (100 MHz, $CDCl_3$): $\delta = 165.1$, 158.0, 153.9, 142.4, 139.1, 134.9, 130.5, 129.4, 128.2, 124.8, 123.1, 122.6, 119.6, 117.2 and 115.1 (aromatic carbons), 101.4 and 101.1 (C-1 and C-1′), 84.7 (C-5 and C-5′), 75.9 (C-4 and C-4′), 71.9, 70.3 and 69.8 (O-*C*H_2-*C*H_2-O *TEG*), 61.6 (C-6), 49.0 (2×N−*C*H_2 *TEG*), 45.3 and 45.2 (4×*C*H_3-*N*-Dans), 35.8 and 35.6 ppm (2×-CH_2-N*C*$H_3$$SO_2$-); ^{31}P NMR (161.98 MHz, $CDCl_3$, 3.0 mM): very broad signal, centred at $\delta = 1.33$ ppm; ^{31}P NMR (161.98 MHz, $CDCl_3$, 0.09 mM): sharp signal at $\delta = 1.5$ ppm; HRMS (MALDI$^-$-TOF): *m*/*z*: calcd for $C_{108}H_{150}N_8O_{36}P_2S_4$: 2324.8511; found: 2323.1221 $[M-H]^-$; 1160.8435 $[M-2H]^{2-}$.

Acknowledgements

We thank the MIUR (PRIN) for grants in support of this investigation and the Centro di Metodologie Chimico-Fisiche (CIMCF), Università di Napoli "Federico II", for the MS and NMR spectroscopy facilities.

[1] For recent reviews, see for example: a) G. W. Gokel, M. M. Daschbach, *Coord. Chem. Rev.* **2008**, *252*, 886–902; b) S. Licen, F. De Riccardis, I. Izzo, P. Tecilla, *Curr. Drug Discovery Technol.* **2008**, *5*, 86–97; c) T. M. Fyles, *Chem. Soc. Rev.* **2007**, *36*, 335–347; d) A. P. Davis, D. N. Sheppard, B. D. Smith, *Chem. Soc. Rev.* **2007**, *36*, 348–357; e) G. W. Gokel, I. A. Carasel, *Chem. Soc. Rev.* **2007**, *36*, 378–389; f) R. S. Hector, M. S. Gin, *Supramol. Chem.* **2005**, *17*, 129–134.

[2] a) R. Dutzler, *Curr. Opin. Struct. Biol.* **2006**, *16*, 439–446; b) R. MacKinnon, *Angew. Chem.* **2004**, *116*, 4363–4376; *Angew. Chem. Int. Ed.* **2004**, *43*, 4265–4277.

[3] For recent reports, see for example: a) W. Wang, R. Li, G. W. Gokel, *Chem. Eur. J.* **2009**, *15*, 10543–10553; b) N. Bernier, S. Carvalho, F. Li, R. Delgado, V. Félix, *J. Org. Chem.* **2009**, *74*, 4819–4827; c) I. Izzo, S. Licen, N. Maulucci, G. Autore, S. Marzocco, P. Tecilla, F. De Riccardis, *Chem. Commun.* **2008**, 2986–2988; d) R. Ferdani, R. Li, R. Pajewski, J. Pajewska, R. K. Winter, G. W. Gokel, *Org. Biomol. Chem.* **2007**, *5*, 2423–2432; e) V. Gorteau, G. Bollot, J. Mareda, S. Matile, *Org. Biomol. Chem.* **2007**, *5*, 3000–3012.

[4] *Essentials of Glycobiology* (Eds.: A. Varki, R. Cumming, J. Esko, H. Freeze, G. Hart, J. Marth), Cold Spring Harbor Laboratory Press, Cold Spring Harbor, **1999**, Chapter 1–21, pp. 1–331.

[5] For recent reports, see for example: a) J. M. Benito, M. Gómez-García, C. Ortiz Mellet, I. Baussanne, J. Defaye, J. M. Garcia Fernández, *J. Am. Chem. Soc.* **2004**, *126*, 10355–10363; b) J. Ni, H. Song, Y. Wang, N. M. Stamatos, L.-X. Wang, *Bioconjugate Chem.* **2006**, *17*, 493–500; c) S. G. Gouin, E. Vanquelef, J. M. Garcia Fernández, C. Ortiz Mellet, F.-Y. Dupradeau, J. Kovensky, *J. Org. Chem.* **2007**, *72*, 9032–9045; d) E. A. B. Kantchev, C.-C. Chang, S. F. Cheng, A.-C. Roche, D.-K. Chang, *Org. Biomol. Chem.* **2008**, *6*, 1377–1385; e) X. Ning, J. Guo, M. A. Wolfert, G.-J. Boons, *Angew. Chem.* **2008**, *120*, 2285–2287; *Angew. Chem. Int. Ed.* **2008**, *47*, 2253–2255.

[6] a) G. Di Fabio, A. Randazzo, J. D'Onofrio, C. Ausìn, A. Grandas, E. Pedroso, L. De Napoli, D. Montesarchio, *J. Org. Chem.* **2006**, *71*, 3395–3408; b) J. D'Onofrio, C. Coppola, G. Di Fabio, L. De Napoli, D. Montesarchio, *Eur. J. Org. Chem.* **2007**, 3849–3858.

[7] C. Coppola, V. Saggiomo, G. Di Fabio, L. De Napoli, D. Montesarchio, *J. Org. Chem.* **2007**, *72*, 9679–9689.
[8] S. Licen, C. Coppola, J. D′Onofrio, D. Montesarchio, P. Tecilla, *Org. Biomol. Chem.* **2009**, *7*, 1060–1063.
[9] For a recent review on fluorescent chemosensors, see: F. Mancin, E. Rampazzo, P. Tecilla, U. Tonellato, *Chem. Eur. J.* **2006**, *12*, 1844–1854.
[10] For applications of dansyl groups in recognition/sensing systems, see for example: a) B. Branchi, P. Ceroni, V. Balzani, G. Bergamini, F. G. Klaerner, F. Voegtle, *Chem. Eur. J.* **2009**, *15*, 7876–7882; b) M. Montalti, L. Prodi, N. Zaccheroni, G. Battistini, S. Marcuz, F. Mancin, E. Rampazzo, U. Tonellato, *Langmuir* **2006**, *22*, 5877–5881; c) S. Pagliari, R. Corradini, G. Galaverna, S. Sforza, A. Dossena, M. Montalti, L. Prodi, N. Zaccheroni, R. Marchelli, *Chem. Eur. J.* **2004**, *10*, 2749–2758; d) A. Ueno, A. Ikeda, I. Ikeda, T. Ikeda, F. Toda, *J. Org. Chem.* **1999**, *64*, 382–387.
[11] a) L. You, G. W. Gokel, *Chem. Eur. J.* **2008**, *14*, 5861–5870; b) L. You, R. Li, G. W. Gokel, *Org. Biomol. Chem.* **2008**, *6*, 2914–2923; c) W. M. Leevy, G. M. Donato, R. Ferdani, W. E. Goldman, P. H. Schlesinger, G. W. Gokel, *J. Am. Chem. Soc.* **2002**, *124*, 9022–9023; d) E. Abel, G. E. M. Maguire, O. Murillo, I. Suzuki, S. L. De Wall, G. W. Gokel, *J. Am. Chem. Soc.* **1999**, *121*, 9043–9052; e) M. K. Mathew, R. Nagaraj, P. Balaram, *J. Biol. Chem.* **1982**, *257*, 2170–2176.
[12] For a recent review, see: M. Köhn, R. Breinbauer, *Angew. Chem.* **2004**, *116*, 3168–3178; *Angew. Chem. Int. Ed.* **2004**, *43*, 3106–3116.
[13] For recent reports, see: a) H. C. Kolb, M. G. Finn, K. B. Sharpless, *Angew. Chem.* **2001**, *113*, 2056–2075; *Angew. Chem. Int. Ed.* **2001**, *40*, 2004–2021; b) V. D. Bock, H. Hiemstra, J. H. van Maarseveen, *Eur. J. Org. Chem.* **2006**, 51–68.
[14] For recent synthetic elaborations of TEG-based linkers, see for example: a) H. Herzner, H. Kunz, *Carbohydr. Res.* **2007**, *342*, 541–557; b) H. T. Uyeda, I. L. Medintz, J. K. Jaiswal, S. M. Simon, H. Mattoussi, *J. Am. Chem. Soc.* **2005**, *127*, 3870–3878.
[15] For a recent example see W. Wang, A. D. Q. Li, *Bioconjugate Chem.* **2007**, *18*, 1036–1052.
[16] S. Rumney IV, E. T. Kool, *J. Am. Chem. Soc.* **1995**, *117*, 5635–5646.
[17] This reagent has been previously described for the synthesis of a mannose–fluorescein conjugate in: C. R. Bertozzi, M. D. Bednarski, *J. Org. Chem.* **1991**, *56*, 4326–4329; the authors recovered it in 44% overall yields. Its synthesis, achieved in 5 steps with 50% yield, and use has been also more recently reported, in: C. Höltke, A. von Wallbrunn, K. Kopka, O. Schober, W. Heindel, M. Schaefers, C. Bremer, *Bioconjugate Chem.* **2007**, *18*, 685–694; another remarkable example of desymmetrized tetraethylene glycol linker is in: A. W. Schwabacher, J. W. Lane, M. W. Schiesher, K. M. Leigh, C. W. Johnson, *J. Org. Chem.* **1998**, *63*, 1727–1729.
[18] Y. Erkan, I. Czolkos, A. Jesorka, L. M. Wilhelmsson, O. Orwar, *Langmuir* **2007**, *23*, 5259–5263.
[19] X. Wu, Y. Wu, L. Hai, Y. Bao, *Lett. Org. Chem.* **2006**, *3*, 911–914.
[20] H. Wang, W.-H. Chan, *Tetrahedron* **2007**, *63*, 8825–8830.
[21] F. Peri, F. Nicotra, C. P. Leslie, F. Micheli, P. Seneci, C. Marchioro, *J. Carbohydr. Chem.* **2003**, *22*, 57–71.
[22] a) R. E. Stafford, T. Fanni, E. A. Dennis, *Biochemistry* **1989**, *28*, 5113–5120; b) P. Babu, D. Chopra, T. N. Guru Row, U. Maitra, *Org. Biomol. Chem.* **2005**, *3*, 3695–3700.
[23] a) M. Vaccaro, A. Accardo, D. Tesauro, G. Mangiapia, D. Loef, K. Schillen, O. Soederman, G. Morelli, L. Paduano, *Langmuir* **2006**, *22*, 6635–6643; b) A. Vergara, L. Paduano, R. Sartorio, *J. Phys. Chem. B* **2001**, *105*, 328–334; c) G. Mangiapia, C. Coppola, G. Vitiello, G. D'Errico, L. De Napoli, A. Radulescu, D. Montesarchio, L. Paduano, unpublished results.
[24] N. Sakai, S. Matile, *J. Phys. Org. Chem.* **2006**, *19*, 452–460.
[25] D. D. Lasic, *Liposomes from Physics to Applications*, Elsevier, Amsterdam, **1993**.
[26] C. Reichardt, *Solvents and Solvent Effects in Organic Chemistry*, 3rd ed., Wiley-VCH, Weinheim, **2003**.
[27] A. K. Covington, F. S. Bates, R. A. Durst, *Pure Appl. Chem.* **1985**, *57*, 531–542.
[28] T. P. Russell, J. S. Lin, S. Spooner, G. D. Wignall, *J. Appl. Crystallogr.* **1988**, *21*, 629–638.
[29] G. D. Wignall, F. S. Bates, *J. Appl. Crystallogr.* **1987**, *20*, 28–40.
[30] B. J. Berne, R. Pecora, *Dynamic Light Scattering with Applications to Chemistry, Biology, and Physics*, Dover, New York, **1975**.
[31] G. A. Brehm, V. A. Bloomfield, *Macromolecules* **1975**, *8*, 663–665.

Received: March 9, 2010
Revised: July 26, 2010
Published online: November 4, 2010

